Pharmaceutica Analytica Acta
ISSN: 2153-2435

Yadav et al., Pharm Anal Acta 2015, 6:10
DOI: 10.4172/2153-2435.1000439

Research Article Open Access

Raman and IR Spectral and DFT Based Vibrational and Electronic Characterization of Isolated and Zwitterionic Forms of L-Tyrosine

Yadav RA[1]*, Dixit V[1], Yogesh M[2] and Santhosh C[2]

[1]*Laser and Spectroscopy Laboratory, Department of Physics, Banaras Hindu University, Varanasi -221005(UP), India*

[2]*Department of Atomic and Molecular Physics, Manipal University, Manipal-576104 (Karnatak), India*

Abstract

Comparative structural and vibrational investigations in two different forms of the L-Tyrosine (L-TYR) have been carried out using Raman and IR spectral and DFT methods. For the optimized structures of the most stable conformers the vibrational assignments of the experimental IR and Raman bands have been proposed using the results of the DFT-B3LYP computations and the PEDs computed using GAR2PED software. The optimized geometrical structures of the molecule belong to the C1 point group in the zwitterionic and isolated forms of the molecule. Possibility of the charge transfer phenomena in the molecule has been investigated in light of the HOMO–LUMO analysis. The electron density mappings of the iso-surfaces with the molecular electrostatic potential (MEP) have been carried out to obtain the different information associated with the size, shape, charge density distribution and site of chemical reactivity of the molecule. On the basis of the NBO analysis presence of intramolecular H bonding and intramolecular charge transfer (ICT) have been proposed.

Keywords: Optimized Geometry; IR and Raman spectra; Frontier orbitals; MEP; NBO; L-Tyrosine; vibrational assignments

Introduction

L-Tyrosine (L-TYR), is one of the essential amino acids and an important component of various food products like milk, fish, cheese, peanuts, almonds, chicken, etc. It acts as a potent anti-depressant agent and also enhances the cellular strength of immune systems in the human body. The phenolic-OH group in the tyrosine molecule is essential for stimulating the antibacterial activity. It is precursor of number of hormones and neurotransmitters [1]. In recent years much attention is being paid towards investigations of the natural and safer antioxidant compounds due to their crucial roles in the food, cosmetics and pharmaceutical products [2]. Also, these compounds enhance the shelf life and are used for prevention of the age related diseases by retarding the process of the lipid per-oxidation and chain reaction [3].

L-TYR helps to regulate the mood, stimulate the nervous system and support the creation of the neurotransmitters including the dopamine, nor-epinephrine and epinephrine [4]. These amino acids also play essential role in the synthesis of melanin which protects against harmful effects of the UV radiations [5] and, also found to be used for the treatment of the allergies, headaches and Parkinson's disease. Their usefulness for the normal functioning of the thyroid, pituitary, and adrenal glands is crucial for living bodies. Thus, L-TYR can affect the health, together with the other amino acids, it may have very important effects, in the people facing dementia, including Alzheimer's disease and it may also reduce the adverse effects of the environmental, psychosocial, and physical stress [6-9]. Recently, some researches about tyrosine and its enzymes have been carried out using molecular dynamics simulations [10-12]. In recent years, the crystal and molecular structures of L-TYR [13,14] and also numerous enzymes associated with tyrosine, e.g., tyrosine phosphatise [15-19] have been investigated. Several workers [4,6,20-24] have investigated the tyrosine molecule and its derivatives using different spectroscopic techniques. However, detailed structural and vibrational characteristics of the L-TYR molecule have been investigated by Contreras et al. [6]. But, Contreras et al. [6] assigned only the functional group modes and only few of the skeletal modes (finger print modes) and excluded the explanation of the weak IR band at 2075 cm^{-1}. Also, HOMO-LUMO orbitals and electron density and molecular electroscopic potentials plots and contours studies, which provide important information about the reactivity, hardness and other characteristics of the molecule, do not appear to have been investigated so far.

Therefore, in the present article we have computed the optimized structural parameters, natural, APT and Mulliken atomic charges and the fundamental vibrational frequencies along with the IR intensities, Raman activities and depolarization ratios of the Raman bands employing the DFT-B3LYP method using the 6-311++G** basis set (Gaussian-09 software) [25,26] for the lowest energy conformers of L-TYR. The experimentally observed IR and Raman frequencies have been analysed with the help of visualization of the form of the normal mode using the Gauss View software and the corresponding PEDs available from the GAR2PED software [25-29]. Reactivity of the title molecule was investigated using the HOMO-LUMO analysis and their orbital energies, molecular electrostatic potential. The natural bond orbital analysis (NBO) analysis has also been carried out.

Computational Details

The geometrical structure of the most stable conformer of ethyl benzene was optimized with the help of the Gauss View 5.0 and

***Corresponding author:** Yadav RA, Laser and Spectroscopy Laboratory, Department of Physics, Banaras Hindu University, Varanasi -221005(UP), India, Tel: +91 542 2368593; Fax: +91 542 2368390; E-mail: rayadav@bhu.ac.in, ray1357@gmail.com

Santhosh C, Department of Atomic and Molecular Physics, Manipal University, Manipal-576104 (Karnatak), India, Tel: 0820-2925071, E-mail: santhosh.cls@manipal.edu

Received August 13, 2015; **Accepted** October 08, 2015; **Published** October 12, 2015

Citation: Yadav RA, Dixit V, Yogesh M, Santhosh C (2015) Raman and IR Spectral and DFT Based Vibrational and Electronic Characterization of Isolated and Zwitterionic Forms of L-Tyrosine. Pharm Anal Acta 6: 439. doi:10.4172/21532435.1000439

Gaussian 09 software as elaborated in ref. [25-28]. By replacing the two H-atoms of the CH_3 group with the $-NH_2$ and -COOH moieties the resulting structures were again optimized. The minimum energy structure corresponds to the most stable structure of L- Phenylalanine (L-PHAL). With this structure of L-PHAL by replacing the H atom of the para position relative to the side carbon chain by an OH group we again optimized the structures and selected the minimum energy structure which is the desired structures of L-TYR (Figure 1). The relative and total energies of the most probable conformers have been presented in Table 1 (zwitterionic form) and Table 2 (isolated form). The vibrational spectrum and related parameters have been investigated in isolated as well as zwitterionic forms of the most stable conformer of L-TYR (Figure 1) (replacing the –COOH and $–NH_2$ groups by the $-CO_2$ and $–NH_3$ groups and optimize again).

The unscaled B3LYP/6-311++G** vibrational wave numbers are usually slightly larger than those of the observed values; therefore, for the sake of the reasonable frequency matching we employed the quantum chemical scaling [30]. The assignments of all the normal modes of vibration have been proposed with the help of the PEDs, calculated using the GAR2PED software [25-29] and with the help of Gauss View software by observing the modes of vibration corresponding to the computed fundamentals.

The molecular electrostatic potential (MEP) surfaces predict the sites, the relative reactivity towards the electrophilic attack, the biological recognition and the hydrogen bonding interactions. The NBO analysis has also been carried out to investigate the intra-molecular charge transfer (CT) interactions, re-hybridisation, the delocalization of electron density (ED) and also second order perturbation theory of molecular orbitals within the present molecule in both the situations.

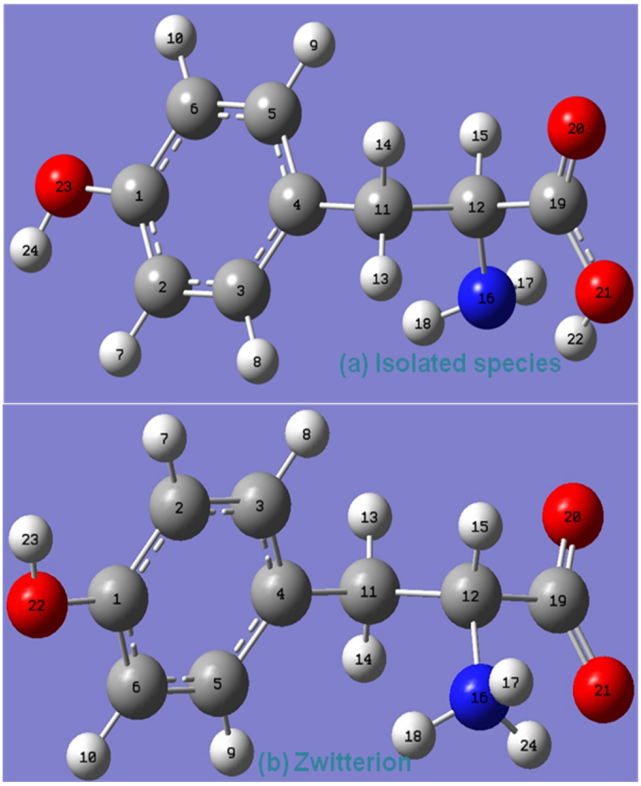

Figure 1: Optimized structures of lowest energy conformers of the isolated and zwitterionic form of L Tyrosine molecule.

Experimental Detail

The compound L- Tyrosine was purchased from the Sigma Aldrich Chemical Co. (USA). A little amount (1-2 mg) of pure, lyophilized powder of L-TYR, was used to record the Raman spectra using a home assembled micro-Raman spectrometer employing Horiba Jobin-Yuon Spectrometer (iHR-320) system with an inverted microscope (Nikon Eclipse Ti-U, Japan). A Diode laser (Star Bright Diode Laser, Torsana Laser Tech, Denmark) λ785 nm was used as the source to illuminate the sample sandwiched between quartz cover slip and borosilicate glass slide. The sample was mounted on the microscope stage and a 60X microscope objective (a converging lens) was used to focus the laser beam and to collect the Raman signals. A liquid nitrogen cooled Symphony CCD detector was employed to collect the Raman scattered radiations. The spectral range of the Raman spectrum was 200-3100 cm^{-1} with the resolution 5 cm^{-1} and accuracy 2 cm^{-1} at spectrometer slit width 100μm. In order to achieve a better Raman spectra data were obtained using a laser power of 47 mW with the acquisition times of 4 min.

FTIR spectrum of L-TYR sample was recorded using KBr pellet. 10 mg of the sample was properly mixed with 990 mg KBr. A pellet from this mixture was made applying appropriate pressure for thirty minutes. FTIR spectrum was recorded using the above pellet at around 23°C temperatures, using an FTIR spectrometer (Jasco 6300) with a standard source. The spectra were recorded in the range 400- 4000 cm^{-1}. We have taken 200 scans with 2 cm^{-1} spectral resolution.

Results and Discussion

Molecular geometry

Front and side views of the geometrical structures of L-TYR have been given in the figure 1. Table 1 contains all the geometrical parameters of L-TYR. It is to be noted that the bond lengths computed at the B3LYP/6-311++G** level appear to be slightly larger in isolated molecule as compared to the observed ones while in zwitterionic form some bond lengths are larger while others are shorter than those of the observed values [6,31]. The atoms C_1, C_2, C_3, C_4, C_5, C_6, C_{11}, H_7, H_8, H_9, H_{10}, O_{23} and H_{24} are coplanar with the phenyl ring plane. The atoms C_{11} and C_{12} are tetrahedrally connected to the atoms C_4, C_{12}, H_{13}, H_{14} and C_{19}, C_{11}, N_{16}, H_{17} respectively, the L-TYR molecule is found to have no symmetry. The computed and observed CH bond lengths are found to have too large differences (Table 1) for isolated molecule while these agree for zwitterionic form. In the phenyl ring, CC bond lengths associated with the C atom directly attached to the side chain with two functional groups are larger, significantly in zwitterionic form, than the other phenyl ring CC bond lengths. Clearly, the lengths of CC σ-bonds in the side chain are much larger compared to the CC bond lengths in the phenyl ring. The C_4-C_{11} bond has been found to be the shortest while the C_{11}-C_{12} bond in isolated and C_{12}-C_{19} bond in zwitterion have been found the largest of all the CC σ-bonds in the side chain of the optimized L-TYR molecule (Figure 1). The O_{23}-H_{24} bond length in isolated form is found to be the shortest of all the bonds (Table 3). In zwitterionic form, the bond containing H_{24} atom is exceptionally larger than those of other two NH bonds of the NH_3 group (Table 3). The computed bond angles are almost in agreement with the observed data, except those which are either associated with the functional groups or with the higher electronegative atoms. The bond angle α(O_{20}-C_{19}-O_{21}) is the largest angle in the molecule. It is interesting to note that the differences between the computed and observed bond angles α(H_{15}-C_{12}-N_{16}), α(C_{12}-N_{16}-H_{18}), α(O_{20}-C_{19}-O_{21}), α(C_{12}-C_{19}-O_{21}), α(C_{11}-C_{12}-C_{19}), α(C_{12}-C_{19}-O_{20}) and α(C_{12}-C_{11}-H_{14}) are 5.3, 3.8, 3.3, 2.9, 2.8, 2.4 and

Con.	E_T (Hartree)	E_R					μ (Debye)	Point Group
		Hartree	($x10^{-2}$) eV	Cal/mole	cm^{-1}	Kelvin		
C-1	-630.22675940	0.00000	0.0	0.0	0.0	0.000000	12.9889	C_1
C-2	-630.22631622	0.00044318	1.206	278.10	97.267	139.946	14.6863	C_1
C-3	-630.22326532	0.00349408	9.508	2192.569	766.862	1103.350	12.1899	C_1

Con. →Conformer, E_T → Total energy, E_R → Relative energy and μ →Dipole moment.

Table 1: Total and relative energies of the possible conformers of zwitterionic L-TYR.

Con.	E_T (Hartree)	E_R					Point Group
		Hartree	($x10^{-2}$) eV	Kcal/mole	cm^{-1}	Kelvin	
C-1	-630.21003038	0.00000	0.0	0.0	0.0	0.000000	C_1
C-2	-630.20763457	0.00239581	6.52	1.5034	525.82	756.54	C_1
C-3	-630.2075066	0.00252378	6.87	1.5837	553.90	796.95	C_1
C-4	-630.20734022	0.00269016	7.32	1.6881	590.42	849.49	C_1
C-5	-630.20656242	0.00346796	9.44	2.1762	761.13	1095.10	C_1
C-6	-630.20637205	0.00368533	10.03	2.3126	808.84	1163.74	C_1
C-7	-630.20591794	0.00411294	11.19	2.5809	902.68	1298.77	C_1
C-8	-630.20549309	0.00453729	12.35	2.8472	995.82	1432.77	C_1
C-9	-630.20499927	0.00503111	13.69	3.1571	1104.20	1588.71	C_1
C-10	-630.20417585	0.00585453	15.93	3.6738	1284.92	1848.72	C_1
C-11	-630.20161342	0.00841646	22.90	5.2814	1847.20	2657.72	C_1
C-12	-630.19973750	0.01029288	28.01	6.4589	2259.03	3250.26	C_1
C-13	-630.19862017	0.01141021	31.05	7.1600	2504.25	3603.08	C_1
C-14	-630.19794310	0.01208728	32.89	7.5849	2652.85	3816.89	C_1
C-15	-630.19568471	0.01434567	39.04	9.0020	3148.51	4530.03	C_1

Con. → Conformer, E_T → Total energy, E_R → Relative energy.

Table 2: Thermo-molecular parameters of the conformer (C-1) of zwitterionic L-TYR.

Parameters (Bond lengths, Angles)	B3LYP Values (Computed)		Observed Values	
	Isolated	Zw	Ref.-31	Ref.-6
$r(C_1\text{-}C_2)$	1.393	1.398	1.382	--
$r(C_1\text{-}C_6)$	1.397	1.394	1.374	--
$r(C_1\text{-}O_{22})$	1.368	1.369	--	1.367
$r(C_2\text{-}C_3)$	1.396	1.391	1.391	--
$r(C_2\text{-}H_7)$	1.086	1.085	0.950	--
$r(C_3\text{-}C_4)$	1.397	1.401	--	1.398
$r(C_3\text{-}H_8)$	1.086	1.085	--	1.085
$r(C_4\text{-}C_5)$	1.403	1.400	1.390	--
$r(C_4\text{-}C_{11})$	1.512	1.515	--	1.539
$r(C_5\text{-}C_6)$	1.388	1.394	1.388	--
$r(C_5\text{-}H_9)$	1.086	1.086	0.950	--
$r(C_6\text{-}H_{10})$	1.083	1.084	0.950	--
$r(C_{11}\text{-}C_{12})$	1.548	1.539	--	1.539
$r(C_{11}\text{-}H_{13})$	1.095	1.092	--	1.088
$r(C_{11}\text{-}H_{14})$	1.092	1.094	--	1.094
$r(C_{12}\text{-}H_{15})$	1.095	1.088	--	1.094
$r(C_{12}\text{-}N_{16})$	1.472	1.512	--	1.488
$r(C_{12}\text{-}C_{19})$	1.541	1.564	--	1.529
$r(N_{16}\text{-}H_{17})$	1.015	1.020	--	1.015
$r(N_{16}\text{-}H_{18})$	1.015	1.022	--	1.048
$r(N_{16}\text{-}H_{24})$	--	1.045	--	--
$r(C_{19}\text{-}O_{20})$	1.203	1.243	--	1.242
$r(C_{19}\text{-}O_{21})$	1.342	1.261	--	1.259
r(OH)/OH	0.963	0.965	--	0.981
r(OH)/COOH	0.983	--	--	--
$\alpha(C_2\text{-}C_1\text{-}C_6)$	119.7	119.8	120.9	--
$\alpha(C_2\text{-}C_1\text{-}O_{22})$	123.0	122.5	--	121.8
$\alpha(C_6\text{-}C_1\text{-}O_{22})$	117.3	117.6	--	117.9
$\alpha(C_1\text{-}C_2\text{-}C_3)$	119.8	119.8	119.9	--
$\alpha(C_1\text{-}C_2\text{-}H_7)$	120.2	120.0	120.1	--

α(C_3-C_2-H_7)	120.0	120.1	120.1	--
α(C_2-C_3-C_4)	121.4	121.3	121.1	--
α(C_2-C_3-H_8)	118.9	118.7	119.5	--
α(C_4-C_3-H_8)	119.7	119.9	119.5	--
α(C_3-C_4-C_5)	117.7	117.9	118.2	--
α(C_3-C_4-C_{11})	121.4	121.2	120.7	--
α(C_5-C_4-C_{11})	120.9	120.9	120.9	--
α(C_4-C_5-C_6)	121.6	121.5	120.8	--
α(C_4-C_5-H_9)	119.5	119.6	119.6	--
α(C_6-C_5-H_9)	118.9	118.8	119.6	--
α(C_1-C_6-C_5)	119.8	119.6	120.1	--
α(C_1-C_6-H_{10})	119.0	119.5	119.9	--
α(C_5-C_6-H_{10})	121.2	120.8	119.9	--
α(C_4-C_{11}-C_{12})	113.4	114.2	--	114.5
α(C_4-C_{11}-H_{13})	109.8	110.7	109.6	--
α(C_4-C_{11}-H_{14})	110.6	109.7	109.6	--
α(C_{12}-C_{11}-H_{13})	108.6	106.1	109.6	--
α(C_{12}-C_{11}-H_{14})	107.2	109.1	109.6	--
α(H_{13}-C_{11}-H_{14})	107.0	106.8	108.1	--
α(C_{11}-C_{12}-H_{15})	108.4	110.5	107.4	--
α(C_{11}-C_{12}-N_{16})	111.1	111.0	--	110.8
α(C_{11}-C_{12}-C_{19})	108.3	111.5	--	111.1
α(H_{15}-C_{12}-N_{16})	112.7	107.8	107.4	--
α(H_{15}-C_{12}-C_{19})	106.5	109.8	107.4	--
α(N_{16}-C_{12}-C_{19})	109.6	106.1	111.2	--
α(C_{12}-N_{16}-H_{17})	111.4	112.4	--	--
α(C_{12}-N_{16}-H_{18})	111.2	113.5	107.4	--
α(C_{12}-N_{16}-H_{24})	--	102.8	--	--
α(H_{17}-N_{16}-H_{18})	107.1	107.8	--	108.2
α(H_{17}-N_{16}-H_{24})	--	108.4	--	--
α(H_{18}-N_{16}-H_{24})	--	111.7	--	--
α(C_{12}-C_{19}-O_{20})	122.8	116.0	125.2	--
α(C_{12}-C_{19}-O_{21})	114.1	114.9	--	117.0
α(O_{20}-C_{19}-O_{21})	123.1	129.1	--	126.4
α(C_{19}-O_{21}-H_{22})/COOH	105.4	--	--	--
α(C_1-O_{22}-H_{23})	109.9	110.1	--	111.1
δ(C_6-C_1-C_2-C_3)	-0.2	-0.1	--	--
δ(C_6-C_1-C_2-H_7)	179.3	179.7	--	--
δ(O_{22}-C_1-C_2-C_3)	-179.9	-179.9	--	--
δ(O_{22}-C_1-C_2-H_7)	-0.4	-0.1	--	--
δ(C_2-C_1-C_6-C_5)	0.3	0.1	--	--
δ(C_2-C_1-C_6-H_{10})	-179.3	-179.6	--	--
δ(O_{22}-C_1-C_6-C_5)	-180.0	-179.9	--	--
δ(O_{22}-C_1-C_6-H_{10})	0.5	0.2	--	--
δ(C_2-C_1-O_{22}-H_{23})	1.1	0.8	--	--
δ(C_6-C_1-O_{22}-H_{23})	-178.6	-179.0	--	--
δ(C_1-C_2-C_3-C_4)	-0.1	-0.0	--	--
δ(C_1-C_2-C_3-H_8)	178.9	179.6	--	--
δ(H_7-C_2-C_3-C_4)	-179.6	-179.8	--	--
δ(H_7-C_2-C_3-H_8)	-0.6	-0.1	--	--
δ(C_2-C_3-C_4-C_5)	0.4	0.1	--	--
δ(C_2-C_3-C_4-C_{11})	-179.1	-179.6	-177.8	--
δ(H_8-C_3-C_4-C_5)	-178.6	-179.5	--	--
δ(H_9-C_3-C_4-C_{11})	1.9	0.8	--	--
δ(C_3-C_4-C_5-C_6)	-0.3	-0.1	--	--
δ(C_3-C_4-C_5-H_9)	179.0	179.1	--	--
δ(C_{11}-C_4-C_5-C_6)	179.2	179.6	178.7	--
δ(C_{11}-C_4-C_5-H_9)	-1.5	-1.3	--	--
δ(C_3-C_4-C_{11}-C_{12})	106.8	68.8	--	--
δ(C_3-C_4-C_{11}-H_{13})	-14.9	-50.8	--	--
δ(C_3-C_4-C_{11}-H_{14})	-132.8	-168.4	--	--

$\delta(C_5\text{-}C_4\text{-}C_{11}\text{-}C_{12})$	-72.7	-110.8	--	--
$\delta(C_5\text{-}C_4\text{-}C_{11}\text{-}H_{13})$	165.6	129.5	--	--
$\delta(C_5\text{-}C_4\text{-}C_{11}\text{-}H_{14})$	47.8	12.0	--	--
$\delta(C_4\text{-}C_5\text{-}C_6\text{-}C_1)$	-0.0	-0.0	--	--
$\delta(C_4\text{-}C_5\text{-}C_6\text{-}H_{10})$	179.5	179.7	--	--
$\delta(H_9\text{-}C_5\text{-}C_6\text{-}C_1)$	-179.4	-179.1	--	--
$\delta(H_9\text{-}C_5\text{-}C_6\text{-}H_{10})$	0.2	0.6	--	--
$\delta(C_4\text{-}C_{11}\text{-}C_{12}\text{-}H_{15})$	60.4	-60.9	--	--
$\delta(C_4\text{-}C_{11}\text{-}C_{12}\text{-}N_{16})$	-63.9	58.6	--	---
$\delta(C_4\text{-}C_{11}\text{-}C_{12}\text{-}C_{19})$	175.6	176.7	170.36	--
$\delta(H_{13}\text{-}C_{11}\text{-}C_{12}\text{-}H_{15})$	-177.2	61.3	--	--
$\delta(H_{13}\text{-}C_{11}\text{-}C_{12}\text{-}N_{16})$	58.4	-179.1	--	--
$\delta(H_{13}\text{-}C_{11}\text{-}C_{12}\text{-}C_{19})$	-62.1	-61.1	--	--
$\delta(H_{14}\text{-}C_{11}\text{-}C_{12}\text{-}H_{15})$	-61.9	176.0	--	--
$\delta(H_{14}\text{-}C_{11}\text{-}C_{12}\text{-}N_{16})$	173.7	-64.4	--	--
$\delta(H_{14}\text{-}C_{11}\text{-}C_{12}\text{-}C_{19})$	53.2	53.6	--	---
$\delta(C_{11}\text{-}C_{12}\text{-}N_{16}\text{-}H_{17})$	150.2	-137.0	--	--
$\delta(C_{11}\text{-}C_{12}\text{-}N_{16}\text{-}H_{18})$	30.9	-14.3	--	--
$\delta(C_{11}\text{-}C_{12}\text{-}N_{16}\text{-}H_{24})$	--	106.5	--	--
$\delta(H_{15}\text{-}C_{12}\text{-}N_{16}\text{-}H_{17})$	28.4	-15.9	--	--
$\delta(H_{15}\text{-}C_{12}\text{-}N_{16}\text{-}H_{18})$	-91.0	106.9	--	--
$\delta(H_{15}\text{-}C_{12}\text{-}N_{16}\text{-}H_{24})$	--	-132.3	--	--
$\delta(C_{19}\text{-}C_{12}\text{-}N_{16}\text{-}H_{17})$	-90.1	101.7	--	--
$\delta(C_{19}\text{-}C_{12}\text{-}N_{16}\text{-}H_{18})$	150.5	-135.5	--	--
$\delta(C_{19}\text{-}C_{12}\text{-}N_{16}\text{-}H_{24})$	--	-14.7	--	--
$\delta(C_{11}\text{-}C_{12}\text{-}C_{19}\text{-}O_{20})$	-72.8	69.2	--	---
$\delta(C_{11}\text{-}C_{12}\text{-}C_{19}\text{-}O_{21})$	105.3	-109.6	--	--
$\delta(H_{15}\text{-}C_{12}\text{-}C_{19}\text{-}O_{20})$	43.6	-53.6	--	--
$\delta(H_{15}\text{-}C_{12}\text{-}C_{19}\text{-}O_{21})$	-138.2	127.6	--	--
$\delta(N_{16}\text{-}C_{12}\text{-}C_{19}\text{-}O_{20})$	165.8	-169.8	--	--
$\delta(N_{16}\text{-}C_{12}\text{-}C_{19}\text{-}O_{21})$	-16.0	11.3	--	--
$\delta(C_{12}\text{-}C_{19}\text{-}O_{21}\text{-}H_{22})$/COOH	3.3	--	--	--
$\delta(O_{20}\text{-}C_{19}\text{-}O_{21}\text{-}H_{22})$	-178.5	--	--	--

The bond lengths and angles are measured in units of Å and degrees (^{0}) respectively.

Table 3: Geometrical parameters for C-1 conformer of L-TYR.

2.4 degrees respectively for isolated molecule and 0.4, 6.1, 2.8, 2.1, 0.4, 9.2 and 0.5 degrees respectively in zwitterion. Like bond lengths, one of the bond angles in the NH_3 group is exceptionally larger than the others, this is equivalent to saying that the angle $\alpha(C_{12}\text{-}N_{16}\text{-}H_{24})$ is exceptionally shorter than the other two. Overall, the computed and observed geometrical data have been found in good agreement. The discrepancies, if any, could occur due to experimental errors as well as due to the fact that in the observed data collective effect of all the conformers are expected to contribute simultaneously.

Atomic partial charges

Natural atomic charges: The natural partial atomic charges partially appear on the molecular surface which could predict the entire chemical properties of the molecule [32,33]. Table 4 contains the natural atomic charges at various atomic sites in both the forms of the L-TYR molecule. All the C atoms, except C_1, of the phenyl ring possess negative natural charges having different magnitudes. The C_1 and C_4 atoms possess the highest and lowest magnitudes of natural charges in phenyl ring. The C atom of the $COOH/CO_2$ group possesses the highest positive charge while the other two C atoms possess negative natural atomic charges in which C_{12} has smaller value in the side chain for both the considered forms. The magnitude of natural charge at the N atom is the highest (-0.88414) in isolated molecule while it is sufficiently high (-0.71534) in the zwitterionic form of L-TYR. All the H atoms in the isolated molecule possess positive natural charges of varying magnitudes while in the zwitterion all the H atoms, except H_{22}, possess positive natural charges with varying magnitudes. Clearly, the values of natural charges on the H atoms associated with the ring, directly attached to the side chain and associated with the OH group have been computed to be ~0.20e - 0.22e, ~0.20e - 0.26e and ~0.46e respectively. The two H atoms of the nitro group possess natural charges ~0.37e in the isolated molecule while ~0.414e in the zwitterion; on the other hand H_{22} in the isolated molecule belonging to the COOH group possessing very small natural charge (~0.50e) as compared to that in the zwitterionic form (~0.67e); where H_{22} atom is associated with nitro group. It could be noted that in the isolated molecule the N atom possesses the highest negative natural charge (~ -0.88414e) while in the zwitterionic molecule O_{21} has the highest negative charge (~ -0.76072e).

APT atomic charges: The atomic polarizability tensor (APT) charges are expressed as the sum of the charge and charge flux tensors [34]. Table 4 contains the APT atomic charges at various atomic sites of L-TYR. The C atoms of the ring possess alternately positive and negative ATP charges; both the C atoms at the juxtra positions of the C atom directly attached to the side chain, attain much smaller positive APT charge (0.01e - 0.04e) than those of the other ring C atoms (0.2e). However, the C atom attached with the OH group holds highest positive APT charge (0. 613493e/ 0.812467e) in the ring for isolated / zwitterionic form, while the C atoms belonging to the side

Atom	Atomic partial charges (Isolated)			Atomic partial charges (Zwitterion)		
	APT	Mulliken	Natural	APT	Mulliken	Natural
C_1	0.613493	-0.435352	0.31468	0.812467	-0.470637	0.31493
C_2	-0.150654	-0.047939	-0.27605	-0.204435	-0.028073	-0.26564
C_3	0.009604	-0.358761	-0.19208	0.039308	-0.398504	-0.18162
C_4	-0.076057	1.151327	-0.07589	-0.122508	1.317786	-0.08505
C_5	0.031030	-0.179803	-0.17718	0.029461	-0.277654	-0.20283
C_6	-0.133771	-0.206873	-0.23714	-0.194348	-0.269538	-0.24175
H_7	0.026331	0.147727	0.20294	0.048736	0.195566	0.20523
H_8	0.037415	0.175254	0.20537	0.051569	0.200611	0.20984
H_9	0.042596	0.178566	0.20731	0.051611	0.203054	0.20574
H_{10}	0.054919	0.201684	0.22034	0.065244	0.215356	0.22232
C_{11}	0.137992	-0.834036	-0.39897	0.172302	-0.938486	-0.41689
C_{12}	0.139311	-0.184624	-0.11510	0.173849	-0.306090	-0.10537
H_{13}	-0.016288	0.167633	0.20843	0.000283	0.221867	0.25676
H_{14}	0.001787	0.216132	0.23650	-0.023739	0.203883	0.21498
H_{15}	-0.028309	0.203647	0.20346	0.006561	0.251243	0.21008
N_{16}	-0.518797	-0.438526	-0.88414	-0.488237	-0.145116	-0.71534
H_{17}	0.153285	0.270493	0.37001	0.272411	0.353028	0.41455
H_{18}	0.167789	0.261335	0.37780	0.310837	0.328162	0.41415
C_{19}	1.156077	-0.237381	0.78978	1.677125	-0.043051	0.74312
O_{20}	-0.777492	-0.252935	-0.58933	-1.227794	-0.478450	-0.69520
O_{21}	-0.789743	-0.127142	-0.68590	-1.282249	-0.492382	-0.76072
H_{22}	0.397038	0.292185	0.49854	-0.994466	-0.276041	-0.67002
O_{23}	-0.766120	-0.227448	-0.67111	0.363525	0.303235	0.46933
H_{24}	0.288563	0.264839	0.46772	0.462488	0.330231	0.45942

Charges are taken in units of e.

Table 4: APT and Mulliken atomic charges of the lowest energy conformer of L-TYR.

chain possess positive APT charges with different magnitudes. The C atom of the COOH/ CO_2 group possesses the highest APT atomic charge (1.156077e/ 1.677125e), while the other C sites of the side chain possess -0.138e and -0.173e APT atomic charges in the isolated and zwitterionic forms. All the H atoms in the molecule, except H_{13} and H_{15} in isolated and H_{14} and H_{22} in zwitterion, possess positive APT charges with varying magnitudes. Clearly, H_{14} in isolated and H_{13} in zwitterion possess the smallest magnitude of APT charges (0.001787e/ 0.000283e) while in the two considered species of the molecule amongst all the H atoms, H_{22} possesses the highest magnitude of APT charge (0.397038/ -0.994466e). The N and the three O atoms possess negative APT charges with the magnitudes -0.518797e/ -0.488237e, -0.777492e/ -1.227794e, -0.789743e/ -1.282249e and -0.766120e/ 0.363525e in the isolated/ zwitterionic forms of L-TYR. It is noticeable that the APT charges at the O atoms in the CO_2 group are nearly twice the APT charges at the O atoms in the COOH group while the APT charge at the O atom of the OH group in the isolated molecule has been found to be twice that at the corresponding site in the zwitterionic molecule. The APT charge at H_{22} (0.397038e) in isolated becomes -0.994466e in the zwitterion state. Conclusively, the APT charges are found to vary to large extent at every reactive site when molecule goes from the isolated state to the zwitterionic state.

Mulliken atomic charges: The Mulliken atomic charge calculation plays a crucial role in the application of quantum chemical calculation to the molecular systems because these charges are responsible for the dipole moment, polarizability, electronic structure, and much more characteristics of the molecular systems. The Mulliken atomic charges at all the sites of the most stable conformers of the two species of the L-TYR molecule have been collected in the Table-4, from which it is interesting to notice that all the C atoms as well as the highly electronegative atoms, namely, O and N atoms in the molecule, except C_4 in both and O_{23} in zwitterion, possess negative Mulliken atomic charges with different magnitudes. The largest and smallest values of the Mulliken atomic charge corresponding to the C atoms in the optimized structure are possessed by C_4 1.151327e/ 1.317786e and C_2 -0.047939e/ - 0.028073e in the isolated/ zwitterionic species of the L-TYR. The Mulliken atomic charges for all the H atoms in the molecule, except H_{22} (-0.276041e) in the zwitterion, are positive with different values. The H atoms associated with the ring, attached tetrahedrally to C atoms and pyramidally to N atom, belonging to the COOH group and associated with the OH group possess the Mulliken atomic charges 0.15e to 0.20e/ 0.20e to 0.22e, 0.17e to 0.20e/ 0.22e to 0.25e, 0.26e to 0.27e/ 0.33e to 0.35e and 0.29e, 0.26e/ 0.33e respectively in the isolated/ zwitterionic forms of the molecule. However, H_{22} in the zwitterionic molecule possesses exceptionally high value of Mulliken atomic charge (– 0.276041e). It is noticeable that the values of the Mulliken charges at different sites in zwitterionic form appear to be higher than those at the corresponding sites in the isolated molecule. The electronegative atoms N_{16}, O_{20}, O_{21} and O_{23} possess Mulliken charges -0.438526e/ -0.145116e, -0.252935e/ -0.478450e, -0.127142e/ -0.492382e and -0.227448e/ +0.330231e respectively in the isolated and zwitterionic states of L-TYR.

Vibrational assignments

The L-TYR molecule, consisting of 24 atoms, has 66 normal modes of vibration as detailed in Table 5. The calculated and observed vibrational frequencies along with the corresponding PEDs with proposed vibrational assignments have been collected in Table 6 (isolated molecule) and Table 7 (zwitterion). In Figures 2-5 the experimentally observed and computed IR and Raman spectra in different frequency ranges have been compared.

In the experimental IR spectrum a weak peak is observed at ~2075

S.N.	Modes	Total No.	Symbol	Groups	No. of Modes in Zw/ Iso. Forms)
1	Stretching	24	ν	C-C C-H C-OH O-H CH_2 N-H, NH_2 CO_2/C=O C-N	9 5 1/2 1/2 2 3/2 2/1 1
2	In plane bending@	6	β	C-H C-O C_4-C_{12}	4 1 1
3	Out of plane bending@	6	ϒ	C-H C-O C_4-C_{12}	4 1 1
4	Twisting	6/7	τ	C-C C-OH NH_3/ NH_2 CH_2	3 1/2 1 1
5	Rocking	4/3	ρ, ρ'	NH_3/ NH_2 CH_2 CO_2/ COOH	2/1 1 1
6	Wagging	2/3	ω	CH_2 CO_2/COOH NH_3/NH_2	1 1 0/1
7	Scissoring	2/3	δ	CH_2 CO_2/COOH NH_3/NH_2	1 1 0/1
8	Angle bending	7/8	α	C-C-C C-C-N H-C-N C-O-H	2 2 2 1/2
9	Deformation	3/0	δ, δ'	NH_3/NH_2	3/0
10	Ring planar deformation	3	α	α(R)	3
11	Ring non-planar deformation	3	Φ	Φ(R)	3

Table 5: Normal modes distribution in the most stable conformers of isolated/ zwitterionic form of L-TYR.

Mode	Computed Frequencies		Observed Freq.		PEDs	Mode Assignment
	Unscaled	Scaled	Raman	IR		
$ν_1$	3835(75,134)0.23	3662	-	3430#	$ν(O_{23}$-$H_{24})$(100)	$ν(O_{23}$-$H_{24})$
$ν_2$	3576(24,51)0.75	3415	-	-	$ν_{asym}(NH_2)$(100)	$ν_{asym}(NH_2)$
$ν_3$	3507(12,94)0.13	3349	-	-	$ν_{sym}(NH_2)$(90)-$ν(O_{21}$-$H_{22})$(10)	$ν_{sym}(NH_2)$
$ν_4$	3481(251,115)0.07	3324	3207#	3207	$ν(O_{21}$-$H_{22})$(89)+ $ν(N_{16}$-$H_{18})$(7)	$ν(O_{21}$-$H_{22})$
$ν_5$	3194(4,144)0.22	3050	3061#	3041, 3068#	$ν(C_6$-$H_{10})$(94)	ν(CH)
$ν_6$	3166(9,135)0.16	3024	3042#	3025, 3042#	$ν(C_3$-$H_8)$(65)+ $ν(C_2$-$H_7)$(33)	ν(CH)
$ν_7$	3160(8,48)0.51	3018	3027#	3024#	$ν(C_5$-$H_9)$(92)	ν(CH)
$ν_8$	3149(16,64)0.61	3007	3014#	3014#	$ν(C_2$-$H_7)$(66)-$ν(C_3$-$H_8)$(33)	ν(CH)
$ν_9$	3090(6,50)0.41	2951	2950#	2960, 2962#	$ν_{asym}(CH_2)$(98)	$ν_{asym}(CH_2)$
$ν_{10}$	3043(23,25)0.21	2906	2923#	2931, 2928#	$ν_{sym}(CH_2)$(60)- $ν(C_{12}$-$H_{15})$(39)	$ν_{sym}(CH_2)$
$ν_{11}$	3032(5,116)0.10	2896	2863#	2894, 2864#	$ν(C_{12}$-$H_{15})$(59)+ $ν_{sym}(CH_2)$(40)	$ν(C_{12}$-$H_{15})$
$ν_{12}$	1835(374,15)0.27	1752	-	1630#	$ν(C_{19}$-$O_{20})$(78)	$ν(C_{19}$-$O_{20})$
$ν_{13}$	1663(29,5)0.74	1588	1587, 1590#	1582, 1589#	$δ(NH_2)$(95)	$δ(NH_2)$
$ν_{14}$	1653(49,56)0.52	1579	1567	1579	$ν(C_5$-$C_6)$(20)+ $ν(C_2$-$C_3)$(18)-$ν(C_1$-$C_6)$(10)-$ν(C_3$-$C_4)$(10)+ $α_2$(R)(11)+$β(C_3$-$H_8)$(6)	ν(R)
$ν_{15}$	1629(15,5)0.72	1556	1551, 1531#	1572, 1532#	$ν(C_1$-$C_2)$(24)+ $ν(C_4$-$C_5)$(17)-$ν(C_1$-$C_6)$(16)-$ν(C_3$-$C_4)$(10)- $α_3$(R)(8)	ν(R)
$ν_{16}$	1543(105,2)0.70	1474	1481, 1463#	1453, 1454#	$ν(C_1$-$C_6)$(10)-$ν(C_3$-$C_4)$(10)+$ν(C_1$-$C_2)$(9)-$ν(C_4$-$C_5)$(7)-$β(C_6$-$H_{10})$(10)+$β(C_2$-$H_7)$(14)+$β(C_3$-$H_8)$(12)-$β(C_5$-$H_9)$(13)-$ν(C_1$-$O_{23})$(8)	β(CH)
$ν_{17}$	1489(6,6)0.73	1422	1419, 1414#	1435, 1438#	$δ(CH_2)$(89)	$δ(CH_2)$

ν_{18}	1466(13,0)0.75	1400	-	1417, 1416#	$\nu(C_5\text{-}C_6)(17)+\nu(C_2\text{-}C_3)(16)+\nu(C_4\text{-}C_5)(6)+\beta(C_6\text{-}H_{10})(12)+\beta(C_2\text{-}H_7)(9)\text{-}\beta(C_3\text{-}H_8)(7)\text{-}\alpha(C_1\text{-}O_{23}\text{-}H_{24})(8)$	ν(R)
ν_{19}	1412(433,6)0.61	1348	1365, 1368#	1363, 1367#	$\alpha(C_{19}\text{-}O_{21}\text{-}H_{22})(65)\text{-}\nu(C_1\text{-}C_6)(15)$	$\alpha(C_{19}\text{-}O_{21}\text{-}H_{22})$
ν_{20}	1376(14,21)0.40	1314	1327, 1328#	1332, 1328#	$\alpha(C_{11}\text{-}C_{12}\text{-}H_{15})(23)\text{-}\omega(CH_2)(23)\text{-}\rho(CH_2)(11)\text{-}\nu(C_{11}\text{-}C_{12})(6)$	$\alpha(C_{11}\text{-}C_{12}\text{-}H_{15})$
ν_{21}	1361(30,1)0.58	1300	-	-	$\beta(C_5\text{-}H_9)(11)+\beta(C_3\text{-}H_8)(10)\text{-}\alpha(C_1\text{-}O_{23}\text{-}H_{24})(11)\text{-}\alpha(N_{16}\text{-}C_{12}\text{-}H_{15})(10)+\nu(C_2\text{-}C_3)(9)\text{-}\nu(C_1\text{-}C_2)(8)\text{-}\nu(C_5\text{-}C_6)(7)\text{-}\nu(C_3\text{-}C_4)(6)\ \nu(C_3\text{-}C_4)(6)+\nu(C_1\text{-}C_6)(6)+\omega(CH_2)(6)$	β(CH)
ν_{22}	1358(19,9)0.32	1297	-	1286#	$\alpha(N_{16}\text{-}C_{12}\text{-}H_{15})(27)\text{-}\omega(CH_2)(25)+\beta(C_5\text{-}H_9)(7)$	$\alpha(N_{16}\text{-}C_{12}\text{-}H_{15})$
ν_{23}	1344(3,4)0.46	1284	1284, 1286#	1267	$\alpha(C_{11}\text{-}C_{12}\text{-}H_{15})(14)+\nu(C_3\text{-}C_4)(9)\text{-}\nu(C_4\text{-}C_5)(8)+\nu(C_5\text{-}C_6)(5)+\beta(C_2\text{-}H_7)(8)+\beta(C_6\text{-}H_{10})(8)+\alpha(N_{16}\text{-}C_{12}\text{-}H_{15})(8)+\rho(CH_2)(6)$	ν(R)
ν_{24}	1292(4,1)0.67	1234	-	1247, 1246#	$\omega(CH_2)(22)+\rho(NH_2)(21)+\alpha(N_{16}\text{-}C_{12}\text{-}H_{15})(12)+\alpha(C_{11}\text{-}C_{12}\text{-}H_{15})(11)$	$\omega(CH_2)$
ν_{25}	1288(4,14)0.25	1230	1249, 1247#	1243	$\alpha(N_{16}\text{-}C_{12}\text{-}H_{15})(24)\text{-}\rho(CH_2)(16)+\alpha(C_{11}\text{-}C_{12}\text{-}H_{15})(14)\text{-}\rho(NH_2)(11)$	$\rho(CH_2)$
ν_{26}	1280(115,12)0.03	1222	1214, 1212#	1214, 1213#	$\nu(C_1\text{-}O_{23})(47)\text{-}\alpha_1(R)(9)\text{-}\nu(C_2\text{-}C_3)(8)+\beta(C_2\text{-}H_7)(8)$	$\nu(C_1\text{-}O_{23})$
ν_{27}	1225(2,27)0.09	1170	1164, 1178#	1176, 1177#	$\nu(C_4\text{-}C_{11})(39)\text{-}\alpha_1(R)(13)\text{-}\nu(C_2\text{-}C_3)(6)\text{-}\nu(C_3\text{-}C_4)(6)\text{-}\nu(C_4\text{-}C_5)(6)$	ν(R)
ν_{28}	1210(18,7)0.73	1156	1156, 1150#	1155, 1153#	$\nu(C_{19}\text{-}O_{21})(33)\text{-}\nu(C_{12}\text{-}C_{19})(16)+\rho(CH_2)(13)+\alpha(C_{19}\text{-}O_{21}\text{-}H_{22})(8)\text{-}\delta(COOH)(6)+\rho(COOH)(6)+\omega(NH_2)(6)$	$\nu(C_{19}\text{-}O_{21})$
ν_{29}	1195(3,4)0.31	1141	-	-	$\beta(C_2\text{-}H_7)(26)\text{-}\beta(C_3\text{-}H_8)(18)\text{-}\beta(C_6\text{-}H_{10})(17)\text{-}\beta(C_5\text{-}H_9)(16)+\nu(C_2\text{-}C_3)(7)$	β(CH)
ν_{30}	1187(207,12)0.11	1134	1114, 1113#	1113, 1112#	$\alpha(C_1\text{-}O_{23}\text{-}H_{24})(48)+\nu(C_1\text{-}C_6)(15)+\beta(C_6\text{-}H_{10})(8)\text{-}\nu(C_1\text{-}O_{23})(7)\text{-}\nu(C_1\text{-}C_2)(6)$	α(C-OH)/OH
ν_{31}	1160(10,3)0.44	1108	1100, 1098#	-	$\rho(NH_2)(19)\text{-}\rho(CH_2)(18)\text{-}\alpha(C_{11}\text{-}C_{12}\text{-}H_{15})(17)+\nu(C_{19}\text{-}O_{21})(6)$	$\rho(NH_2)$
ν_{32}	1120(20,1)0.66	1070	-	1099, 1099#	$\beta(C_6\text{-}H_{10})(12)\text{-}\beta(C_5\text{-}H_9)(10)+\beta(C_2\text{-}H_7)(9)\text{-}\beta(C_3\text{-}H_8)(7)+\nu(C_2\text{-}C_3)(10)\text{-}\nu(C_5\text{-}C_6)(9)+\nu(C_{12}\text{-}N_{16})(8)$	β(CH)
ν_{33}	1097(14,12)0.54	1048	1045, 1046#	1042, 1046#	$\nu(C_{12}\text{-}N_{16})(39)\text{-}\nu(C_{11}\text{-}C_{12})(15)+\rho(CH_2)(7)\text{-}\beta(C_{12}\text{-}C_{19})(6)$	$\nu(C_{11}\text{-}C_{12})$
ν_{34}	1029(0,0)0.04	983	-	-	$\alpha_1(R)(49)+\nu(C_1\text{-}C_6)(11)+\nu(C_1\text{-}C_2)(10)\text{-}\nu(C_3\text{-}C_4)(7)\text{-}\nu(C_4\text{-}C_5)(7)$	α_1(R)
ν_{35}	979(48,6)0.29	958	986, 985#	986, 988#	$\tau(CH_2)(15)\text{-}\gamma(C_5\text{-}H_9)(14)+\omega(NH_2)(10)+\gamma(C_6\text{-}H_{10})(8)\text{-}\rho(NH_2)(6)\text{-}\omega(NH_2)(6)$	$\tau(CH_2)$
ν_{36}	973(15,2)0.35	952	967#	939, 939#	$\gamma(C_5\text{-}H_9)(37)\text{-}\gamma(C_6\text{-}H_{10})(26)+\tau(CH_2)(6)$	γ(CH)
ν_{37}	948(48,2)0.57	928	935, 938#	929#	$\omega(NH_2)(24)\text{-}\nu(C_{11}\text{-}C_{12})(23)+\gamma(C_3\text{-}H_8)(14)+\nu(C_{12}\text{-}C_{19})(7)$	$\nu(C_{12}\text{-}C_{19})$
ν_{38}	942(7,1)0.74	922	894, 897#	-	$\gamma(C_3\text{-}H_8)(43)\text{-}\gamma(C_2\text{-}H_7)(16)\text{-}\Phi_1(R)(13)$	γ(CH)
ν_{39}	887(22,16)0.02	868	878	896, 899#	$\gamma(C_6\text{-}H_{10})(10)+\alpha(C_4\text{-}C_{11}\text{-}C_{12})(10)+\omega(NH_2)(10)+\gamma(C_2\text{-}H_7)(9)+\omega(COOH)(7)\text{-}\gamma(C_4\text{-}C_{11})(6)$	$\omega(NH_2)$
ν_{40}	874(46,1)0.52	855	855#	878, 878#	$\tau(C_{19}\text{-}O_{21})(33)+\tau(CH_2)(13)\text{-}\nu(C_{12}\text{-}N_{16})(13)\text{-}\omega(NH_2)(10)\text{-}\nu(C_{11}\text{-}C_{12})(8)$	$\nu(C_{12}\text{-}N_{16})$
ν_{41}	855(51,12)0.14	837	845, 846#	842, 842#	$\tau(C_{19}\text{-}O_{21})(36)+\omega(NH_2)(9)\text{-}\tau(CH_2)(7)\text{-}\alpha_2(R)(7)+\nu(C_{12}\text{-}N_{16})(6)$	$\tau(C_{19}\text{-}O_{21})$
ν_{42}	846(20,11)0.04	828	828, 829#	829, 830#	$\omega(NH_2)(21)+\tau(C_{19}\text{-}O_{21})(13)\text{-}\nu(C_{12}\text{-}C_{19})(10)+\alpha_3(R)(8)+\nu(C_1\text{-}O_{23})(7)+\nu(C_1\text{-}C_6)(6)$	ν(R)
ν_{43}	837(29,2)0.09	819	808	803, 808#	$\gamma(C_6\text{-}H_{10})(40)+\gamma(C_5\text{-}H_9)(28)\text{-}\gamma(C_1\text{-}O_{23})(8)$	γ(CH)
ν_{44}	815(25,1)0.17	798	796, 797#	793, 799#	$\gamma(C_2\text{-}H_7)(56)+\gamma(C_3\text{-}H_8)(22)\text{-}\gamma(C_1\text{-}O_{23})(7)$	γ(CH)
ν_{45}	792(14,8)0.09	775	741, 738#	741, 739#	$\alpha_1(R)(17)\text{-}\nu(C_{12}\text{-}C_{19})(12)\text{-}\nu(C_1\text{-}O_{23})(10)\text{-}\delta(COOH)(10)+\nu(C_4\text{-}C_{11})(9)+\omega(COOH)(8)\text{-}\nu(C_{19}\text{-}O_{21})(6)$	ω(COOH)
ν_{46}	730(2,2)0.72	714	-	-	$\Phi_1(R)(60)+\gamma(C_4\text{-}C_{11})(12)\text{-}\gamma(C_1\text{-}O_{23})(12)\text{-}\omega(COOH)(6)$	$\Phi_1(R)$
ν_{47}	702(12,6)0.05	687	714, 714#	713, 715#	$\omega(COOH)(24)+\Phi_1(R)(16)\text{-}\nu(C_4\text{-}C_{11})(10)\text{-}\delta(COOH)(8)\text{-}\nu(C_{11}\text{-}C_{12})(7)\text{-}\alpha_1(R)(7)$	$\nu(C_4\text{-}C_{11})$
ν_{48}	657(3,2)0.66	643	-	646#	$\delta(COOH)(34)+\omega(NH_2)(22)+\Phi_1(R)(10)+\omega(COOH)(10)$	δ(COOH)
ν_{49}	655(1,5)0.75	641	641, 642#	651	$\alpha_3(R)(79)$	α_3(R)
ν_{50}	565(11,2)0.46	553	574, 574#	576, 575#	$\rho(COOH)(16)+\gamma(C_1\text{-}O_{23})(11)+\omega(NH_2)(11)+\alpha(C_{11}\text{-}C_{12}\text{-}N_{16})(10)\text{-}\Phi_2(R)(8)\text{-}\alpha(C_4\text{-}C_{11}\text{-}C_{12})(6)\text{-}\alpha_2(R)(6)$	ρ(COOH)
ν_{51}	526(14,1)0.33	515	528, 534#	530, 535#	$\gamma(C_1\text{-}O_{23})(27)+\gamma(C_4\text{-}C_{11})(13)\text{-}\Phi_2(R)(25)+\delta(COOH)(7)\text{-}\rho(COOH)(7)$	$\Phi_2(R)$
ν_{52}	492(9,3)0.40	481	492, 496#	495, 499#	$\alpha_2(R)(39)+\gamma(C_1\text{-}O_{23})(11)\text{-}\Phi_2(R)(10)$	$\alpha_2(R)$
ν_{53}	428(11,0)0.59	419	-	434, 435#	$\beta(C_1\text{-}O_{23})(46)\text{-}\alpha_3(R)(16)+\beta(C_4\text{-}C_{11})(13)+\Phi_3(R)(11)$	$\beta(C_1\text{-}O_{23})$
ν_{54}	423(3,0)0.35	414	-	408#	$\Phi_3(R)(76)$	$\Phi_3(R)$

ν_{55}	409(4,3)0.32	400	380, 386#	388#	α(C_{11}-C_{12}-N_{16}) (37)+ ω(COOH)(7)- Φ_1(R)(6)	α(N_{16}-C_{12}-C_{11})
ν_{56}	347(7,3)0.58	340	338#	340#	α(C_{11}-C_{12}-N_{16}) (22)+ Φ_1(R)(16)- γ(C_4-C_{11})(10)+ γ(C_1-O_{23})(10)	γ(C_1-O_{23})
ν_{57}	340(8,2)0.28	333	336, 331#	327#	α(N_{16}-C_{12}-C_{19}) (40)- ρ(COOH) (29)	α(N_{16}-C_{12}-C_{19})
ν_{58}	310(96,1)0.71	303	311, 313#	313#	τ(C_1-O_{23})(89)	τ(C_1-O_{23})
ν_{59}	307(15,0)0.74	300	--	--	τ(C_{12}-N_{16})(41)- τ(C_{19}-O_{21})(20)- β(C_4-C_{11})(13)	β(C_4-C_{11})
ν_{60}	296(27,0)0.73	290	-	294#	τ(C_{12}-N_{16})(41)+β(C_4-C_{11})(16)-τ(C_{19}-O_{21})(8)-β(C_{12}-C_{19}) (7)	τ(C_{12}-N_{16})
ν_{61}	186(0,1)0.13	182	196#	-	Φ_2(R)(24)- α(C_{11}-C_{12}-C_{19}) (16)- α(C_4-C_{11}-C_{12})(14)- ν(C_4-C_{11})(6)- γ(C_4-C_{11})(6)- γ(C_{12}-C_{19})(6)	α(C_4-C_{11}-C_{12})
ν_{62}	169(9,1)0.66	165	167#	--	α(C_{11}-C_{12}-C_{19}) (34)+ Φ_2(R)(32)+γ(C_{12}-C_{19})(7)- α(C_4-C_{11}-C_{12})(7)	α(C_{11}-C_{12}-C_{19})
ν_{63}	83(1,1)0.75	81	--	--	τ(C_{12}-C_{19})(58)- τ(C_{12}-N_{16})(14)- τ(C_{19}-O_{21})(10)	τ(C_{12}-C_{19})
ν_{64}	63(1,1)0.71	62	--	--	τ(C_{12}-C_{19})(31)-γ(C_4-C_{11})(14)-α(C_4-C_{11}-C_{12})(12)- Φ_2(R) (9)-τ(C_{12}-N_{16})(9)+α(C_{11}-C_{12}-C_{19}) (7)-τ(C_{19}-O_{21})(6)	γ(C_4-C_{11})
ν_{65}	46(3,1)0.75	45	--	--	τ(C_{11}-C_{12})(46)+ τ(C_{12}-C_{19})(20)- τ(C_{12}-N_{16})(7)	τ(R'')
ν_{66}	40(1,4)0.75	39	--	--	τ(C_4-C_{11})(57)+ τ(C_{12}-C_{19})(18)- τ(C_{12}-N_{16})(9)	τ(R')

The number before the modes are the % potential energy calculated using normal coordinate analysis. The modes contributing with ≤ 5% have been omitted. The abbreviations ν, δ, α(R), Φ_1(R), ν(R), β, γ, α(A-B-C), ω, ρ, τ asym and sym have been used for stretching, scissoring, ring planar deformation, ring non-planar deformation, ring stretching, in plane bending, out of plane bending, angle bending, wagging, rocking, torsion, anti-symmetric and symmetric respectively.
Calculated wave numbers up to 1000 cm^{-1} were scaled by the scale factor 0.9786 and those above 1000 cm^{-1} by the scale factor 0.9550 for larger wave numbers.
Number outside bracket is frequency in cm^{-1} unit, numbers within the bracket are IR intensity (approximate) and Raman activity (approximate) and number outside bracket is depolarization ratio. The values superscripted with # are taken from literature Ref.-[6]

Table 6: Observed and computed IR and Raman frequencies of the normal modes of vibration, PEDs and assignments for the most stable conformer of L-TYR in isolated molecule.

Mode	Computed Frequencies		Observed Freq.		PEDs	Mode Assignment
	Unscaled	Scaled	Raman	IR		
ν_1	3811(144,239)0.34	3640	-	3430#	ν(O_{22}-H_{23})(100)	ν(O_{22}-H_{23})
ν_2	3526(134,72)0.67	3367	-	-	ν_{asym}(H_{17}-N_{16}-H_{18})(100)	ν_{asym}(H_{17}-N_{16}-H_{18})
ν_3	3456(136,226)0.06	3300	3207	3207	ν_{sym}(H_{17}-N_{16}-H_{18}) (99)	ν_{sym}(H_{17}-N_{16}-H_{18})
ν_4	3190(10,360)0.21	3047	-	-	ν(C_6-H_{10})(92) + ν(C_5-H_9)(6)	ν(CH)
ν_5	3174(14,330)0.15	3031	3061#	3041, 3068#	ν(C_3-H_8)(53)+ ν(C_2-H_7)(45)	ν(CH)
ν_6	3161(11,200)0.52	3019	3042#	3025, 3042#	ν(C_5-H_9)(89) - ν(C_6-H_{10})(6)	ν(CH)
ν_7	3159(21,89)0.75	3017	3027#	3024#	ν(C_2-H_7)(53)- ν(C_3-H_8)(42)	ν(CH)
ν_8	3127(44,66)0.30	2986	3014#	3014#	ν(C_{12}-H_{15})(86) - ν(N_{16}-H_{24})(10)	ν(C_{12}-H_{15})
ν_9	3106(414,146)0.06	2966	2950#	2960, 2962#	ν(N_{16}-H_{24})(88) + ν(C_{12}-H_{15})(10)	ν(N_{16}-H_{24})
ν_{10}	3093(6,162)0.64	2954	2923#	2931, 2928#	ν_{asym}(CH_2)(95)	ν_{asym}(CH_2)
ν_{11}	3047(23,299)0.04	2910	2863#	2894, 2864#	ν_{sym}(CH_2)(99)	ν_{sym}(CH_2)
ν_{12}	1669(317,21)0.75	1594	-	1630#	δ_{as}(NH_3)(40)+ ν_{as}(CO_2)(33)- δ'_{as}(NH_3)(16)- ρ_2(NH_3)(5)	δ_{as}(NH_3)
ν_{13}	1659(433,7)0.75	1584	1587, 1590#	1582, 1589#	ν_{as}(CO_2)(53)+δ'_{as}(NH_3)(34)+ ρ(CO_2)(5)	ν_{as}(CO_2)
ν_{14}	1647(78,133)0.56	1573	1567	1579	ν(C_2-C_3)(20)+ν(C_5-C_6)(17)-ν(C_1-C_6) (13)-ν(C_3-C_4)(11)+ α_2(R)(10)-β(C_3-H_8)(7)- β(C_6-H_{10})(5)	ν(R)
ν_{15}	1627(38,29)0.63	1554	1551, 1531#	1572, 1532#	ν(C_1-C_2)(20)+ ν(C_4-C_5)(20)-ν(C_1-C_6)(15)- α_3(R)(8) -ν(C_3-C_4)(7)- β(C_5-H_9)(6)	ν(R)
ν_{16}	1622(84,16)0.65	1549	1481, 1463#	1453, 1454#	δ_{as}(NH_3)(34)+ δ'_{as}(NH_3)(32)+ δ_s(NH_3)(11)+ ν(C_{19}-O_{20})(8)	δ'_{as}(NH_3)
ν_{17}	1538(164,4)0.74	1469	--	1435, 1438#	β(C_2-H_7)(17)+ β(C_3-H_8)(14)- β(C_5-H_9)(12)+ ν(C_3-C_4)(11)- ν(C_1-C_2)(11)- β(C_6-H_{10})(9)- ν(C_1-C_6)(8)+ ν(C_1-O_{22})(7)+ ν(C_4-C_5)(5)	β(CH)
ν_{18}	1486(13,11)0.75	1419	1419, 1414#	1417, 1416#	δ(CH_2)(89)	δ(CH_2)
ν_{19}	1464(28,2)0.75	1398	--	1363, 1367#	ν(C_5-C_6)(19)- β(C_6-H_{10})(13)-ν(C_2-C_3) (13)- α(C-OH) (8)- β(C_2-H_7)(7)+ β(C_3-H_8) (6)+β(C_4-C_{11})(5) + β(C_1-O_{22})(5)+ν(C_4-C_5)(5)	ν(R)
ν_{20}	1423(566,20)0.74	1359	1365, 1368#	1332, 1328#	δ_s(NH_3)(71)- ν(C_{19}-O_{20})(9)- δ_{as}(NH_3)(6)	δ_s(NH_3)
ν_{21}	1393(35,26)0.62	1330	1327, 1328#	-	α(C_{11}-C_{12}-H_{15})(30)- α(H_{15}-C_{12}-N_{16}) (17)- ω(CH_2)(12)+ ρ(CH_2)(9)+ ν(C_{19}-O_{21})(7)	α(C_{11}-C_{12}-H_{15})
ν_{22}	1364(103,4)0.37	1303	-	1286#	β(C_5-H_9)(19)+ β(C_3-H_8)(12)+ ω(CH_2)(11)+ α(C-OH)(10)- α(H_{15}-C_{12}-C_{19})(8)+ β(C_6-H_{10}) (7)	β(CH)
ν_{23}	1360(20,7)0.20	1298	--	1267	ω(CH_2)(16)+ ν(C_2-C_3)(11)+ν(C_4-C_5)(7)+ ν(C_1-C_6)(6)-ν(C_5-C_6)(6)- α(C-OH)(6)- α(H_{15}-C_{12}-C_{19})(6)- ν(C_1-C_2)(6)- β(C_3-H_8)(5) - ν(C_3-C_4)(5)- β(C_5-H_9)(5)	ν(R)

ν_{24}	1344(289,18)0.19	1284	1284, 1286#	1247, 1246#	$\nu_s(CO_2)$(41)- $\delta(CO_2)$(10)- $\alpha(C_{11}$-C_{12}-$H_{15})$(9)+ $\delta_s(NH_3)$(8)- $\nu(C_{12}$-$C_{19})$(8)+ $\alpha(H_{15}$-C_{12}-$N_{16})$ (7)	$\nu_s(CO_2)$
ν_{25}	1332(6,13)0.61	1272	1249, 1247#	1243	$\omega(CH_2)$(19)+ $\nu(C_3$-$C_4)$(11)-$\nu(C_4$-$C_5)$ (10)- $\beta(C_2$-$H_7)$(8)+ $\rho(CH_2)$(5)+ $\nu(C_5$-$C_6)$ (5)-$\nu(C_1$-$C_6)$(5)	$\omega(CH_2)$
ν_{26}	1275(5,33)0.34	1218	1214, 1212#	1214, 1213#	$\alpha(H_{15}$-C_{12}-$N_{16})$ (21)+ $\rho(CH_2)$(17)+ $\alpha(C_{11}$-C_{12}-$H_{15})$(17+ $\omega(CH_2)$(14)	$\alpha(H_{15}$-C_{12}-$N_{16})$
ν_{27}	1268(173,65)0.03	1211	1164, 1178#	1176, 1177#	ν(C-OH)(46)+ α_1(R)(10)- $\nu(C_1$-$C_2)$(9)- $\nu(C_5$-$C_6)$(7)- $\beta(C_3$-$H_8)$(7)- $\beta(C_2$-$H_7)$(5)	ν(C-OH)
ν_{28}	1237(43,3)0.72	1181	--	1155, 1153#	$\rho(CH_2)$(18)- $\alpha(C_{11}$-C_{12}-$H_{15})$ (16)- $\alpha(H_{15}$-C_{12}-$N_{16})$ (8)- $\rho_1(NH_3)$ (8)+ $\rho_2(NH_3)$(7)+ $\nu(C_{11}$-$C_{12})$(7)- $\alpha(C_{11}$-C_{12}-$N_{16})$(5)+ $\nu(C_4$-$C_5)$(5)	ρ(CH2)
ν_{29}	1220(3,82)0.05	1165	1156, 1150#	-	$\nu(C_4$-$C_{11})$(38)- α_1(R)(11) -$\nu(C_3$-$C_4)$ (9)-$\nu(C_5$-$C_6)$(7) - $\nu(C_2$-$C_3)$(5)+ $\omega(CH_2)$(5)- $\beta(C_5$-$H_9)$(5)	ν(R)
ν_{30}	1194(2,7)0.28	1140	1114, 1113#	-	$\beta(C_2$-$H_7)$(29)- $\beta(C_3$-$H_8)$(20)+ $\beta(C_5$-$H_9)$(13)- $\beta(C_6$-$H_{10})$(11)-$\nu(C_2$-$C_3)$(8)- α(C-OH)(6)+ $\nu(C_1$-$C_2)$(5)	β(CH)
ν_{31}	1187(275,30)0.07	1134	1100, 1098#	1113, 1112#	α(C-OH)(46)+ $\nu(C_1$-$C_6)$(16) -$\beta(C_6$-$H_{10})$(13)- $\nu(C_1$-$O_{22})$(10)	α(C-OH)
ν_{32}	1141(34,3)0.66	1090	-	1099, 1099#	$\beta(C_5$-$H_9)$(12)-$\beta(C_6$-$H_{10})$(11)-$\rho_2(NH_3)$ (10) - $\nu(C_5$-$C_6)$(8)+$\rho(CH_2)$(8)-$\nu(C_{11}$-$C_{12})$(7)+ $\rho_1(NH_3)$(7) +$\beta(C_3$-$H_8)$(7)+ $\nu(C_2$-$C_3)$(6) - $\beta(C_2$-$H_7)$(5)	β(CH)
ν_{33}	1112(130,8)0.33	1062	1045, 1046#	1042, 1046#	$\rho_2(NH_3)$(24)+ $\alpha(C_{11}$-C_{12}-$H_{15})$ (8)+ $\alpha(H_{15}$-C_{12}-$C_{19})$(7)+ $\nu(C_{11}$-$C_{12})$(6)-$\nu(C_5$-$C_6)$(6)- $\beta(C_6$-$H_{10})$(6)+ $\alpha(N_{16}$-C_{12}-$C_{19})$(5)- $\nu(C_{12}$-$N_{16})$ (5)	$\rho_2(NH_3)$
ν_{34}	1084(17,6)0.74	1035	1017, 1017#	1016, 1017#	$\rho_1(NH_3)$(30)+ $\rho(CH_2)$(12)+ $\rho_2(NH_3)$(11)+ $\alpha(H_{15}$-C_{12}-$C_{19})$(9)+ $\alpha(N_{16}$-C_{12}-$C_{19})$(7)	$\rho_1(NH_3)$
ν_{35}	1038(38,30)0.50	991	986, 985#	986, 988#	$\nu(C_{12}$-$N_{16})$(30)- $\nu(C_{11}$-$C_{12})$(21)- τ(CH2)(7)+ $\rho_2(NH_3)$(7)+ $\alpha(C_4$-C_{11}-$C_{12})$(6)	$\nu(C_{11}$-$C_{12})$
ν_{36}	1027(2,0)0.12	981	-	939, 939#	α_1(R)(50)+ $\nu(C_1$-$C_2)$(11)+$\nu(C_1$-$C_6)$(10)- $\nu(C_4$-$C_5)$(7)- $\nu(C_3$-$C_4)$(7)- $\beta(C_6$-$H_{10})$(5)	α_1(R)
ν_{37}	979(0,1)0.34	958	935, 938#	-	$\gamma(C_5$-$H_9)$(37)-$\gamma(C_3$-$H_8)$(22) - $\gamma(C_6$-$H_{10})$(20)+ $\gamma(C_2$-$H_7)$(11) +Φ_3(R)(8)	γ(CH)
ν_{38}	956(2,2)0.72	936	894, 897#	-	$\gamma(C_3$-$H_8)$(31)+ $\gamma(C_5$-$H_9)$(19)+ Φ_1(R)(17)- $\gamma(C_2$-$H_7)$(16)- $\gamma(C_6$-$H_{10})$(10)	γ(CH)
ν_{39}	943(20,8)0.49	923	878	896, 899#	τ(CH_2)(29)- $\rho_1(NH_3)$(28)- $\nu(C_{11}$-$C_{12})$(12)+ $\alpha(C_{11}$-C_{12}-$N_{16})$(5)	τ(CH_2)
ν_{40}	896(146,25)0.10	877	855#	878, 878#	$\nu(C_{12}$-$C_{19})$(32)+ $\delta(CO_2)$(10)+ $\rho_2(NH_3)$(10) - $\nu(C_{11}$-$C_{12})$(7)- $\alpha(C_{11}$-C_{12}-$C_{19})$(6)	$\nu(C_{12}$-$C_{19})$
ν_{41}	860(24,20)0.01	842	845, 846#	842, 842#	$\gamma(C_6$-$H_{10})$(16)+ $\nu(C_{12}$-$N_{16})$(12)+ $\gamma(C_2$-$H_7)$ (8)- Φ_2(R)(6)+ $\nu(C_5$-$C_6)$(6)- $\nu(C_{12}$-$C_{19})$(6)+ $\gamma(C_1$-$O_{22})$(5)- $\gamma(C_4$-$C_{11})$(5)	$\nu(C_{12}$-$N_{16})$
ν_{42}	849(12,45)0.09	831	828, 829#	829, 830#	$\gamma(C_6$-$H_{10})$(12)-α_2(R)(11)- $\nu(C_1$-$O_{22})$(8))-$\nu(C_1$-$C_2)$(7)-$\nu(C_1$-$C_6)$(6)- $\nu(C_5$-$C_6)$(5) +$\gamma(C_5$-$H_9)$(6)	ν(R)
ν_{43}	830(12,8)0.54	812	808	803, 808#	$\gamma(C_6$-$H_{10})$(35)+$\gamma(C_5$-$H_9)$(19)- $\gamma(C_2$-$H_7)$(11) - $\nu(C_{12}$-$N_{16})$(9)-$\gamma(C_3$-$H_8)$(6) - τ(CH2)(5)	γ(CH)
ν_{44}	822(57,6)0.11	804	796, 797#	793, 799#	$\gamma(C_2$-$H_7)$(36)+$\gamma(C_3$-$H_8)$(19)- $\nu(C_{12}$-$N_{16})$(10)+ $\gamma(C_1$-$O_{22})$(8)- τ(CH2)(7)	γ(CH)
ν_{45}	806(74,22)0.02	789	741, 738#	741, 739#	$\delta(CO_2)$(25)-α_1(R)(12)+ $\omega(CO_2)$(10)+ $\nu(C_1$-$O_{22})$(10)+ $\nu(C_{11}$-$C_{12})$(6)+ $\nu(C_{12}$-$C_{19})$(5)	$\delta(CO_2)$
ν_{46}	737(5,5)0.64	721	714, 714#	713, 715#	Φ_1(R)(53)+ $\omega(CO_2)$(11)- $\gamma(C_1$-$O_{22})$(11)- $\gamma(C_4$-$C_{11})$(11)	Φ_1(R)
ν_{47}	721(2,6)0.10	706	-	-	Φ_1(R)(29)- $\nu(C_4$-$C_{11})$(11)- $\delta(CO_2)$(11) - α_1(R)(9) - $\omega(CO_2)$(6)- $\gamma(C_1$-$O_{22})$(5)+ $\nu(C_1$-$O_{22})$(5)	$\nu(C_4$-$C_{11})$
ν_{48}	676(13,7)0.44	662	641, 642#	646#	Φ_1(R)(20)+$\delta(CO_2)$(17)- $\omega(CO_2)$(16)+ $\alpha(N_{16}$-C_{12}-$C_{19})$(11)- $\nu(C_{12}$-$C_{19})$(6)+ $\alpha(C_4$-C_{11}-$C_{12})$(6)	$\omega(CO_2)$
ν_{49}	654(1,12)0.71	640	574, 574#	651	α_3(R)(78)+ $\beta(C_1$-$O_{22})$(5)	α_3(R)
ν_{50}	557(6,2)0.48	545	--	576, 575#	$\gamma(C_1$-$O_{22})$(16))- Φ_2(R)(13) +$\rho(CO_2)$ (12) - α_2(R) (10)- $\gamma(C_4$-$C_{11})$(8)+ $\alpha(N_{16}$-C_{12}-$C_{19})$(8) + $\alpha(C_{11}$-C_{12}-$N_{16})$(6) - $\alpha(C_4$-C_{11}-$C_{12})$ (6)	$\gamma(C_4$-$C_{11})$
ν_{51}	522(60,3)0.16	511	528, 534#	530, 535#	$\gamma(C_1$-$O_{22})$(25)-Φ_2(R)(23)-$\gamma(C_4$-$C_{11})$(12)- $\rho(CO_2)$ (11)	$\gamma(C_1$-$O_{22})$
ν_{52}	490(37,3)0.57	480	492, 496#	495, 499#	α_2(R)(37)+ $\gamma(C_1$-$O_{22})$(7)+ $\nu(C_{12}$-$C_{19})$(7)+ $\rho(CO_2)$ (7)-Φ_2(R) (7)	α_2(R)

ν_{53}	426(8,1)0.20	417	455, 457#	434, 435#	Φ_3(R)(38)+β(C_1-O_{22})(29)- α_3(R)(10)-β(C_4-C_{11})(8)	β(C_1-O_{22})
ν_{54}	424(6,0)0.61	415	--	408#	Φ_3(R)(63)- β(C_1-O_{22})(12)	Φ_3(R)
ν_{55}	402(15,8)0.37	393	380, 386#	388#	α(C_{11}-C_{12}-N_{16})(33)+ α(C_{11}-C_{12}-C_{19})(11)-Φ_1(R) (8)+ α_2(R)(5)	α(C_{11}-C_{12}-N_{16})
ν_{56}	341(22,4)0.27	334	338#	340#	α(C_{11}-C_{12}-N_{16})(23)-ρ(CO_2)(10)+Φ_1(R)(8)+α(N_{16}-C_{12}-C_{19})(7)- β(C_4-C_{11})(6)- β(C_1-O_{22})(5)+ γ(C_1-O_{22})(5)	ρ(CO_2)
ν_{57}	329(82,6)0.58	322	336, 331#	327#	α(N_{16}-C_{12}-C_{19})(32)- ρ(CO_2)(16)+ τ(NH_3)(6)-ρ_2(NH_3)(6)+ τ(OH)(6)- γ(C_4-C_{11})(5)	α(N_{16}-C_{12}-C_{19})
ν_{58}	321(159,0)0.74	314	311, 313#	313#	τ(OH)(87)	τ(OH)
ν_{59}	302(4,1)0.75	296	--	--	β(C_4-C_{11})(38)+ β(C_1-O_{22})(12)+ α(C_{11}-C_{12}-N_{16})(7) + τ(R'')(5)+ γ(C_4-C_{11})(5)	β(C_4-C_{11})
ν_{60}	255(26,4)0.41	250	256, 257#	294#	τ(NH_3)(62) + δ'_{as}(NH_3)(12)- α(N_{16}-C_{12}-C_{19})(5)	τ(NH_3)
ν_{61}	183(4,2)0.30	179	196#	--	α(C_{11}-C_{12}-C_{19})(24)-Φ_2(R)(12)+α(C_4-C_{11}-C_{12})(9) + ν(C_{12}-C_{19})(8)+ν(C_4-C_{11}) (7)-ω(CO_2)(6)- α_1(R)(5)	α(C_{11}-C_{12}-C_{19})
ν_{62}	164(36,1)0.74	160	167#	--	Φ_2(R)(41)+α(C_{11}-C_{12}-C_{19})(22)-α(C_4-C_{11}-C_{12})(10)	Φ_2(R)
ν_{63}	77(1,3)0.75	75	--	--	τ(CO_2)(40) - τ(NH_3)(31)+ τ(R') (10)	τ(CO_2)
ν_{64}	62(19,2)0.71	61	--	--	τ(CO_2)(31) - τ(NH_3)(25)-α(C_{11}-C_{12}-C_{19})(11)+α(C_4-C_{11}-C_{12})(7)-γ(C_4-C_{11})(6)+Φ_2(R)(5)	α(C_4-C_{11}-C_{12})
ν_{65}	47(25,4)0.75	46	--	--	τ(R'') (58) + τ(CO_2)(13) - τ(NH_3)(10)+ τ(R') (6)	τ(R'')
ν_{66}	40(8,7)0.75	39	--	--	τ(R') (38)+ τ(CO_2)(15) - τ(NH_3)(14) + γ(C_4-C_{11})(10)- τ(R'')(8)	τ(R')

The number before the modes are the % potential energy calculated using normal coordinate analysis. The modes contributing with ≤ 5% have been omitted. The abbreviations ν, δ, α(R), Φ_1(R), ν(R), β, γ, α(A-B-C), ω, ρ, τ asym and sym have been used for stretching, scissoring, ring planar deformation, ring non-planar deformation, ring stretching, in plane bending, out of plane bending, angle bending, wagging, rocking, torsion, anti-symmetric and symmetric respectively.

Calculated wave numbers up to 1000 cm^{-1} were scaled by the scale factor 0.9786 and those above 1000 cm^{-1} by the scale factor 0.9550 for larger wave numbers.

Number outside bracket is frequency in cm^{-1} unit, numbers within the bracket are IR intensity (approximate) and Raman activity (approximate) and number outside bracket is depolarization ratio. The values superscripted with # are taken from literature Ref.-[6]

Table 7: Observed and computed IR and Raman frequencies of the normal modes of vibration, PEDs and assignments for the most stable conformer of L-TYR in zwitterionic form.

Donor NBOs (i)	Acceptor NBOs (j)	E(2) kcal/mol	E(j) – E(i) (a.u.)	F(i, j) (a.u.)
σ(C_1-C_2)	σ*(C_1-C_6)	4.16	1.27	0.065
π(C_1-C_2)	π*(C_3-C_4)	21.63	0.30	0.072
π(C_1-C_2)	π*(C_5-C_6)	16.56	0.30	0.063
σ(C_2-C_3)	σ*(C_1-O_{23})	4.43	1.05	0.061
π(C_3-C_4)	π*(C_1-C_2)	17.85	0.28	0.064
π(C_3-C_4)	π*(C_5-C_6)	20.93	0.29	0.069
σ(C_3-H_8)	σ*(C_4-C_5)	4.59	1.09	0.063
σ(C_5-C_6)	π*(C_1-C_2)	22.07	0.28	0.071
σ(C_5-C_6)	π*(C_3-C_4)	18.33	0.29	0.066
σ(C_5-H_9)	σ*(C_3-C_4)	4.57	1.10	0.063
σ(C_6-H_{10})	σ*(C_1-C_2)	4.04	1.08	0.059
σ(C_{11}-H_{13})	σ*(C_4-C_5)	4.42	1.07	0.061
σ(C_{11}-H_{14})	σ*(C_{12}-N_{16})	4.03	0.82	0.051
σ(O_{21}-H_{22})	σ*(C_{19}-O_{20})	6.45	1.38	0.084
σ(O_{23}-H_{24})	σ*(C_1-C_6)	4.27	1.30	0.067
CR(1) O_{20}	RY*(1) C_{19}	7.14	19.88	0.338
LP(1) N_{16}	σ*(C_{12}-H_{15})	5.05	0.74	0.055
LP(1) N_{16}	σ*(C_{12}-C_{19})	4.40	0.70	0.050
LP(1) N_{16}	σ*(O_{21}-O_{22})	10.34	0.74	0.079
LP(1) O_{20}	RY*(1) C_{19}	17.90	1.74	0.158
LP(2) O_{20}	σ*(C_{12}-C_{19})	19.05	0.60	0.097
LP(2) O_{20}	σ*(C_{19}-O_{21})	31.61	0.63	0.128
LP(1) O_{21}	σ*(C_{12}-C_{19})	4.73	0.96	0.061
LP(2) O_{21}	π*(C_{19}-O_{20})	48.56	0.34	0.116
LP(1) O_{23}	σ*(C_1-C_2)	6.04	1.17	0.075
LP(2) O_{23}	π*(C_1-C_2)	27.68	0.35	0.094
π*(C_1-C_2)	π*(C_3-C_4)	266.58	0.01	0.079
π*(C_1-C_2)	π*(C_5-C_6)	289.41	0.01	0.082

Table 8: Second order perturbation theory analysis of Fock Matrix in the NBO basis of L-TYR (Isolated Molecule).

Donor NBOs (i)	Acceptor NBOs (j)	E(2) kcal/mol	E(j) – E(i) (a.u.)	F(i, j) (a.u.)
$\sigma(C_1-C_2)$	$\sigma^*(C_1-C_6)$	4.13	1.27	0.065
$\sigma(C_2-C_3)$	$\sigma^*(C_1-O_{22})$	4.26	1.05	0.060
$\pi(C_2-C_3)$	$LP^*(1)C_1$	53.69	0.14	0.094
$\pi(C_2-C_3)$	$LP(1)C_4$	41.08	0.15	0.088
$\sigma(C_3-H_8)$	$\sigma^*(C_4-C_5)$	4.60	1.09	0.063
$\pi(C_5-C_6)$	$LP^*(1)C_1$	54.09	0.13	0.093
$\pi(C_5-C_6)$	$LP(1)C_4$	44.40	.15	0.090
$\sigma(C_5-H_9)$	$\sigma^*(C_3-C_4)$	4.62	1.09	0.063
$\sigma(C_6-H_{10})$	$\sigma^*(C_1-C_2)$	4.08	1.07	0.059
$\sigma(C_{11}-H_{13})$	$\sigma^*(C_{12}-N_{16})$	5.44	0.73	0.056
$\sigma(C_{11}-H_{14})$	$\sigma^*(C_3-C_4)$	4.57	1.07	0.062
$\sigma(O_{22}-H_{23})$	$\sigma^*(C_1-C_6)$	4.28	1.30	0.067
$CR(1)\ O_{21}$	$RY^*(1)\ C_{19}$	4.09	19.94	0.256
$LP^*(1)\ C_1$	$\pi^*(C_2-C_3)$	61.01	0.15	0.104
$LP^*(1)\ C_1$	$\pi^*(C_5-C_6)$	62.06	0.15	0.105
$LP(1)\ C_4$	$\pi^*(C_2-C_3)$	77.03	0.13	0.109
$LP(1)\ C_4$	$\pi^*(C_5-C_6)$	75.71	.14	0.108
$LP(1)\ C_4$	$\sigma^*(C_{11}-C_{12})$	5.74	.48	0.064
$LP(1)\ O_{20}$	$RY^*(1)\ C_{19}$	9.63	1.78	0.117
$LP(2)\ O_{20}$	$\sigma^*(C_{12}-C_{19})$	20.63	0.55	0.095
$LP(2)\ O_{20}$	$\sigma^*(C_{19}-O_{21})$	20.31	0.77	0.114
$LP(1)\ O_{21}$	$RY^*(1)\ C_{19}$	8.90	1.79	0.113
$LP(2)\ O_{21}$	$\sigma^*(C_{12}-C_{19})$	16.37	0.58	0.088
$LP(2)\ O_{21}$	$\sigma^*\ (N_{16}-H_{24})$	14.22	0.54	0.080
$LP(2)\ O_{21}$	$\sigma^*\ (C_{19}-O_{20})$	17.87	0.85	0.114
$LP(3)\ O_{21}$	$\pi^*(C_{19}-O_{20})$	95.87	0.27	0.143
$LP(1)\ O_{22}$	$\sigma^*(C_1-C_2)$	5.99	1.16	0.075
$LP(2)\ O_{22}$	$LP^*(1)C_1$	49.41	0.20	0.118

Table 9: Second order perturbation theory analysis of Fock Matrix in the NBO basis of L-TYR (Zwitterionic).

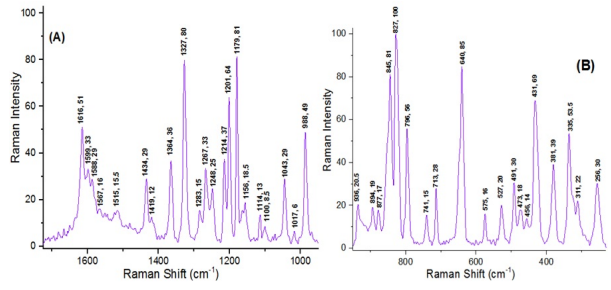

Figure 2: Observed Raman spectrum of the L-TYR.

cm^{-1} which appears to be arising due to some combination or overtone mode. The intense Raman peak observed at 1327 cm^{-1}, assigned to the symmetric CO_2 stretching mode, seems to give rise to the IR peak at ~2075 cm^{-1} in combination with the CO_2 scissoring mode. Thus the presence of 2075 cm^{-1} appears to be one of the signatures of the existence of the molecule in the zwitterionic form. These observations inspired us to investigate the vibrational spectra of isolated as well as zwitterionic form of L-TYR. The normal mode assignments could be discussed under the following three sections: (i) phenyl ring modes (30), (ii) OH group modes (3) and (iii) side carbon chain modes (33).

Phenyl Ring Modes [30]: The ring stretching modes ν(R) have been identified at the computed frequencies 1579 (ν_{14}), 1556 (ν_{15}), 1400 (ν_{18}), 1284 (ν_{23}), 1170(ν_{27}) and 828 (ν_{42}) cm^{-1} in isolated molecule while these have been observed in zwitterion at frequencies 1573 (ν_{14}), 1554 (ν_{15}), 1398 (ν_{19}), 1298 (ν_{23}), 1165 (ν_{29}) and 831 (ν_{42}) cm^{-1}. The ring stretching modes had been assigned at the frequencies 1618, 1572, 1296, 1235, 1126 and 1003 cm^{-1} by Layton et al. [35] in zwitterionic

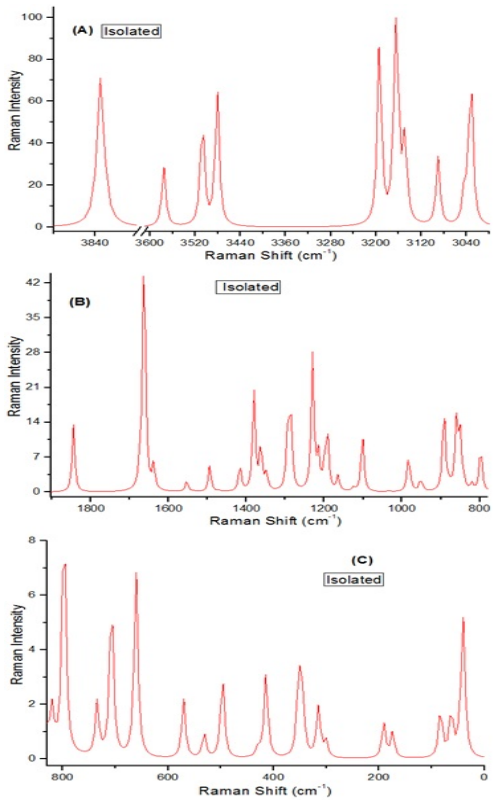

Figure 3(a): Computed Raman spectrum of the isolated molecule of L-TYR.

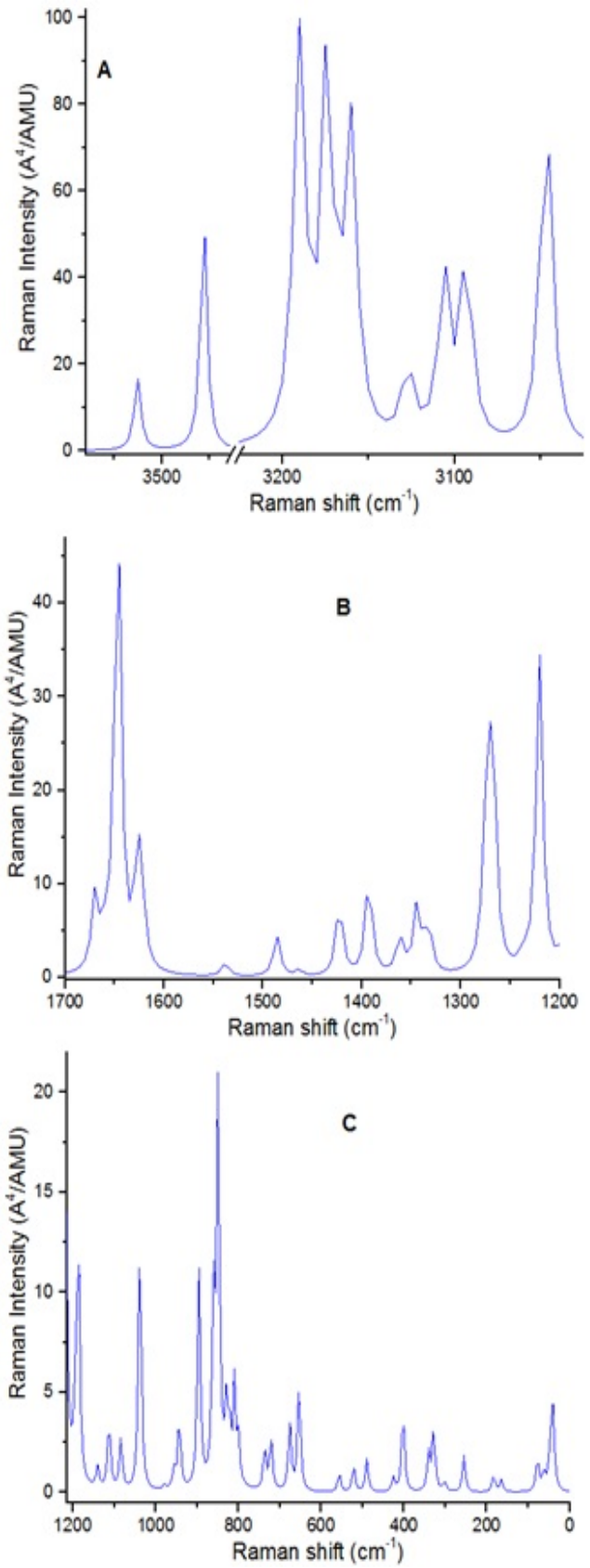

Figure 3(b): Computed Raman spectrum of the zwitterion of L-TYR.

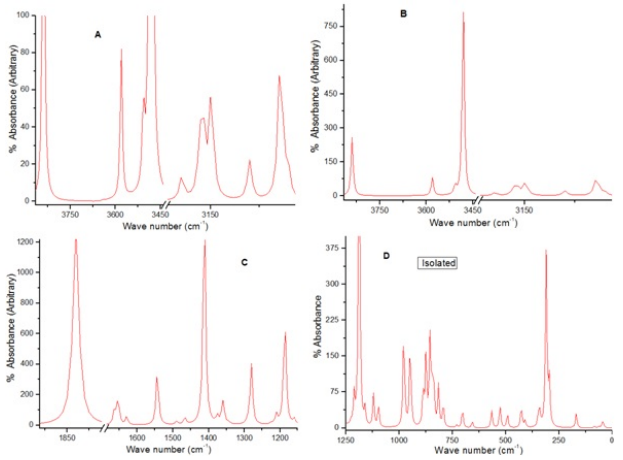

Figure 4(a): Computed IR spectrum of the isolated molecule of L-TYR.

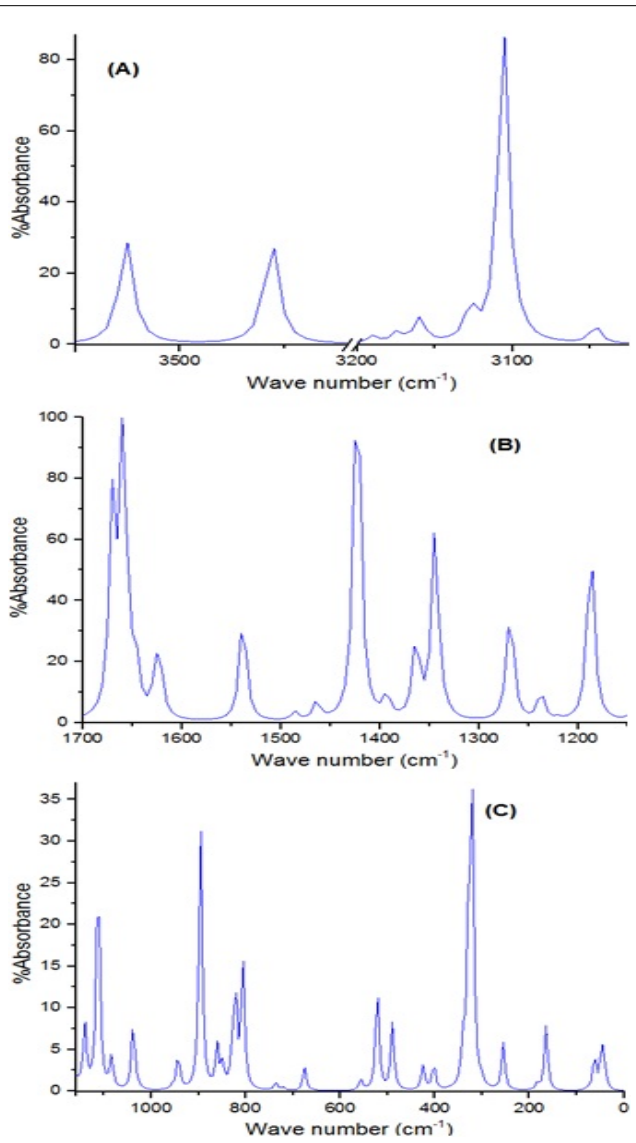

Figure 4(b): Computed IR spectrum of the zwitterion of L-TYR.

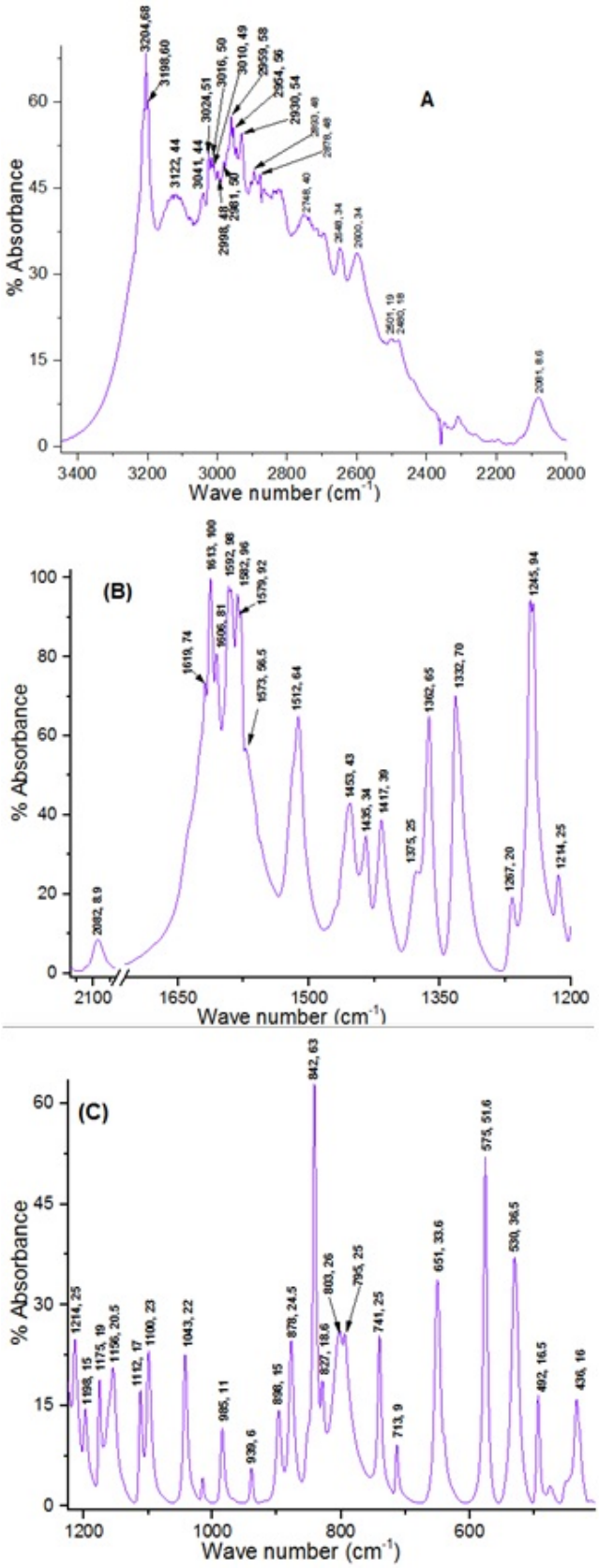

Figure 5: Experimentally observed IR spectrum of the L-TYR.

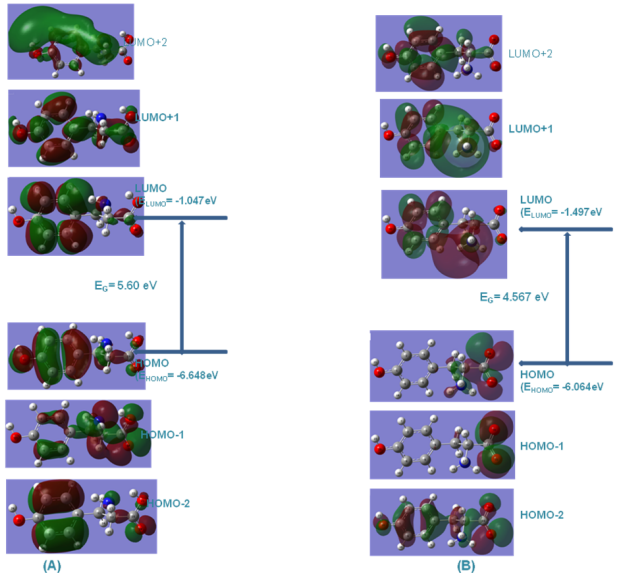

Figure 6: The atomic orbital compositions of the frontier MO of (A) Isolated species and (B) Zwitterion of the L-Tyrosine.

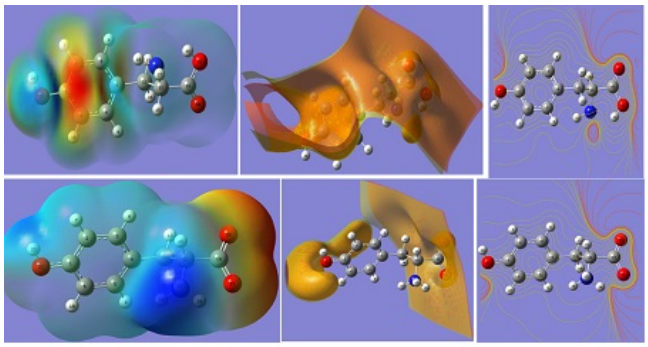

Figure 7: Total density mappings, MEP mappings and MEP arrays of isolated species (upper) and zwitterion of L-TYR.

LTRYP; at 1722, 1661, 1640, 1517, 1396 and 937 cm^{-1} by Contreras et al. [6] in zwitterionic L-Tyrosine (L-TYR) and at 1565, 1546, 1455, 1269, 1052 and 1000 cm^{-1} by Dixit et al. [36] in zwitterionic L-Phenylalanine (LPHAL) respectively. These modes are generally coupled with the other modes. For isolated molecule, the ring planar deformation modes $\alpha_1(R)$, $\alpha_3(R)$ and $\alpha_2(R)$ have been computed to be 983 (ν_{34}), 641(ν_{49}) and 481(ν_{52}) cm^{-1} while in zwitterionic form they correspond to the frequencies 981 (ν_{36}), 640(ν_{49}) and 480 (ν_{52}) cm^{-1}, corresponding to the frequencies 876, 552 and 445 cm^{-1} in zwitterionic L-TRYP [Layton et al. Ref. [35]]; 949, 606 and 361 cm^{-1} in zwitterionic L-TYR [Contreras et al. Ref. [6]] and also 968, 620 and 572 cm^{-1} in zwitterionic L-PHAL [Dixit et al. Ref. [36]]; all of these modes are coupled with the other modes. The three ring non-planar deformation modes $\Phi_1(R)$, $\Phi_2(R)$ and $\Phi_3(R)$, which were assigned at the frequencies 742, 569 and 420 cm^{-1} by Layton et al. [35] in zwitterionic L-TRYP; at 659, 490 and 402 cm^{-1} by Contreras et al. [6] in zwitterionic L-TYR and at 749, 406 and 232 cm^{-1} by Dixit et al. [36] in zwitterionic L-PHAL respectively, are correlated to the frequencies 714(ν_{46}), 515(ν_{51}) and 414(ν_{54}) cm^{-1} in isolated species while in zwitterionic form they have been correlated to

the frequencies 721(ν_{46}), 415(ν_{54}) and 160 (ν_{62}) cm^{-1} corresponding to modes 4 and 16(a,b) of the benzene molecule. These have been found to couple with many deformations, however few α(R) and Φ(R) modes are pure and localized.

The CH stretching modes $\nu(C_2\text{-}H_7)$, $(C_5\text{-}H_9)$, $\nu(C_3\text{-}H_8)$ and $\nu(C_6\text{-}H_{10})$ have been assigned at the frequencies 3007 (ν_8), 3018(ν_7), 3024(ν_6) and 3050(ν_5) cm^{-1} respectively in isolated form and at the frequencies 3017 (ν_7), 3019(ν_6), 3031(ν_5) and 3047(ν_4) cm^{-1} respectively in zwitterionic form. The ν(C-H) modes were assigned at 3057, 3045, 3035and 3024 cm^{-1} by Layton et al. [35] in zwitterionic L-TRYP; at 2941, 2940, 2939 and 2939 cm^{-1} by Contreras et al. [6] in zwitterionic L-TYR and also at 3048, 3037, 3029 and 3018 cm^{-1} by Dixit et al.[36] in zwitterionic L-PHAL respectively. The C-H stretching vibrations are pure and highly localized modes, however, they are found to occur in association with one another. The $\nu(C_1\text{-}O_{23})$ and $\nu(C_4\text{-}C_{12})$ modes occur at frequencies 1222 (ν_{26}) and 687 (ν_{47}) cm^{-1} in isolated molecule while in zwitterion they have been assigned at the frequencies 1268 (ν_{27}) and 706 (ν_{47}) cm^{-1}, these modes are also coupled with many other modes.

The CH planar deformation modes $\beta(C_6\text{-}H_{10})$, $\beta(C_3\text{-}H_8)$, $\beta(C_5\text{-}H_9)$ and $\beta(C_2\text{-}H_7)$ have been found to correspond to the frequencies 1070(ν_{32}), 1141(ν_{29}) 1300(ν_{21}) and 1474(ν_{16}) cm^{-1} respectively in isolated molecule while to the frequencies 1090(ν_{32}), 1140(ν_{30}) 1303(ν_{22}) and 1469(ν_{17}) cm^{-1} respectively in zwitterionic molecule. The frequencies, 1531, 1454, 1441 and 1275 cm^{-1}, were assigned to the CH planar deformation modes in zwitterionic form of L-TRYP by Layton et al. [35]. For zwitterionic L-TYR only three frequencies 1213, 1069 and 1051 cm^{-1} were assigned to the CH planar deformation modes by Contreras et al. [6], which seems to be incomplete assignment. The frequencies 1412, 1304, 1290, 1145 and 1124 cm^{-1}, were assigned to the CH planar deformation modes by Dixit et al [36]. in zwitterionic L-PHAL respectively. These modes appear in strong association with other many modes. The CH non-planar deformation modes $\gamma(C_5\text{-}H_9)$, $\gamma(C_3\text{-}H_8)$, $\gamma(C_6\text{-}H_{10})$ and $\gamma(C_2\text{-}H_7)$ have been found dominantly in the frequencies 952(ν_{36}), 922(ν_{38}), 819(ν_{43}) and 798(ν_{44}) cm^{-1} respectively in isolated form of molecule while in zwitterion these have been observed at the frequencies 958(ν_{37}), 936(ν_{38}), 812(ν_{43}) and 804(ν_{44}) cm^{-1} respectively corresponding to the frequencies 965, 916, 854 and 753 cm^{-1} by Layton et al. [35] in zwitterionic L-TRYP; 1122, 1108, 902 and 891 cm^{-1} by Contreras et al. [6] in zwitterionic L-TYR and 966, 950, 894, 844 and 700 cm^{-1} by Dixit et al. [36] in zwitterionic L-PHAL respectively . The modes $\beta(C_4\text{-}C_{11})$, $\gamma(C_4\text{-}C_{11})$, $\beta(C_1\text{-}O_{23})$ and $\gamma(C_1\text{-}O_{23})$ correspond to the frequencies 300(ν_{59}), 62(ν_{64}), 419(ν_{53}) and 340(ν_{56}) cm^{-1} respectively in isolated molecule while these modes have been calculated to be 296(ν_{59}), 545(ν_{50}), 417(ν_{53}) and 511(ν_{51}) cm^{-1} respectively in zwitterion, which are also coupled with other modes.

OH group modes: The OH group attached directly to the phenyl ring at the site C_1 is associated with three normal modes of the vibrations; OH stretching mode -$\nu(O_{23}\text{-}H_{24})$, COH angle bending mode -$\alpha(C_1\text{-}O_{22}\text{-}H_{23})$ and OH torsion mode -$\tau(C_1\text{-}O_{22})$ which have been assigned in the present case for isolated molecule at the frequencies 3662(ν_1), 1134(ν_{30}) and 303(ν_{58}) cm^{-1} and for the zwitterionic form at 3640(ν_1), 1134(ν_{31}) and 314 (ν_{58}) cm^{-1} respectively, corresponding to the earlier assigned frequencies 3557, 943 and 290 cm^{-1}[6] respectively. The stretching and torsion modes are pure and highly localized while bending mode occurs in association with the other modes.

Carbon chain modes: The side carbon chain attached to the C_4 atom of the phenyl ring (Figure 1) is associated with 33 normal modes of vibration. The twisting modes $\tau(C_4\text{-}C_{12})$, $\tau(C_{12}\text{-}C_{13})$, corresponding to the frequencies 31 and 66 cm^{-1} [35] in zwitterionic L-TRYP; 28 and 87 cm^{-1} [6] in zwitterionic L-TYR and 33 and 49 cm^{-1} [36] in zwitterionic L-PHAL, have been found in isolate and zwitterion at the frequencies 39(ν_{66}), 45 (ν_{65}) cm^{-1} and 39(ν_{66}), 46 (ν_{65}) cm^{-1}. The angle bending modes $\alpha(C_{11}\text{-}C_{12}\text{-}C_{19})$, $\alpha(C_4\text{-}C_{11}\text{-}C_{12})$, $\alpha(N_{16}\text{-}C_{12}\text{-}C_{19})$, $\alpha(N_{16}\text{-}C_{12}\text{-}C_{11})$, $\alpha(N_{16}\text{-}C_{12}\text{-}H_{15})$ and $\alpha(C_{11}\text{-}C_{12}\text{-}H_{15})$ correspond to the frequencies 165(ν_{62}), 182(ν_{61}), 333(ν_{57}), 400(ν_{55}), 1297(ν_{22}) and 1314(ν_{20}) cm^{-1} respectively for isolated species while they have been found for zwitterion at the frequencies 179(ν_{61}), 61 (ν_{64}), 322(ν_{57}), 393(ν_{55}), 1218(ν_{26}) and 1330(ν_{21}) cm^{-1} respectively. The stretching modes $\nu(C_{12}\text{-}C_{19})$, $\nu(C_{11}\text{-}C_{12})$, $\nu(C_{12}\text{-}N_{16})$ and $\nu(C_{12}\text{-}H_{15})$ have been computed to be 928 (ν_{37}), 1048 (ν_{33}), 855 (ν_{40}) and 2896(ν_{11}) cm^{-1} and 877 (ν_{40}), 991(ν_{35}), 842 (ν_{41}) and 2986(ν_8) cm^{-1} respectively for isolated and zwitterion L-TYR molecule. All of these modes, except $\nu(C_{12}\text{-}H_{15})$, have been found to couple with a number of vibrational modes. The $\nu(C_{12}\text{-}H_{15})$ mode have been found localized and pure. These stretching modes were assigned by Layton et al. [35] in zwitterionic L-TRYP at the frequencies 582, 988, 770 and 2942 cm^{-1}; Contreras et al. [6] assigned these modes in zwitterionic L-TYR at the frequencies 823, 1140, 1024 and 2826 cm^{-1} while for zwitterionic L-PHAL Dixit et al.[36] assigned these modes at 875, 992, 809 and 2983 cm^{-1}.

6.3.3.1 COOH/ CO_2 group modes: In the isolated L-TYR molecule, the COOH group is associated with the stretching modes $\nu(O_{21}\text{-}H_{22})$, $\nu(C_{19}\text{-}O_{20})$ and $\nu(C_{19}\text{-}O_{21})$ which have been assigned at the frequencies 3324(ν_4), 1752(ν_{12}) and 1156 (ν_{28}) cm^{-1}, which were found at 3302, 1800 and 862 cm^{-1} by Govindarasu et al. [31], respectively while the anti-symmetric and symmetric stretching of CO_2 group in zwitterion, $\nu_{as}(CO_2)$ and $\nu_s(CO_2)$, have been assigned at the frequencies 1584(ν_{13}) and 1284(ν_{24}) cm^{-1}, which were already found corresponding to the frequencies 1688 and 1290 cm^{-1} by Layton et al. [35] in zwitterionic L-TRYP; at 1757 and 1557 cm^{-1} by Contreras et al. [6] in zwitterionic L-TYR and also at 1594 and 1283 cm^{-1} by Dixit et al. [36] in zwitterionic L-PHAL. The OH stretching mode is highly localised and pure but the later are coupled with other modes. The angle bending mode $\alpha(C_{19}\text{-}O_{21}\text{-}H_{22})$ and the OH torsion mode $\tau(C_{19}\text{-}O_{21})$ of COOH Group have been assigned at the frequencies 1348(ν_{19}) and 837(ν_{41}) cm^{-1}. These modes were found already by Govindarasu et al. [31] at 1387 and 862 cm^{-1}. The first one is highly localised while the later is coupled with other modes. The modes $\tau(C_{12}\text{-}C_{19})$, ω(COOH), ρ(COOH) and δ(COOH) have been assigned at the frequencies 81(ν_{63}), 775(ν_{45}), 553(ν_{50}) and 643(ν_{48}) cm^{-1} respectively in isolated molecule while the modes $\tau(C_{12}\text{-}C_{19})$, $\omega(CO_2)$, $\rho(CO_2)$ and $\delta(CO_2)$ have been assigned at the frequencies 75(ν_{63}), 662(ν_{48}), 334(ν_{56}) and 789(ν_{45}) cm^{-1} respectively in zwitterion, all of these have been found to be coupled with other modes. These modes had already been assigned at the frequencies 61, 847, 503 and 819 cm^{-1} by Layton et al. [35]; at 36, 677, 452 and 609 cm^{-1} by Contreras et al. [6] in zwitterionic L-TYR and also at 65, 662, 506 and 735 cm^{-1} by Dixit et al. [36] in zwitterionic L-PHAL respectively.

NH_2/ NH_3 group modes: In isolated L-TYR molecule there are six modes of vibration due to the NH_2 group, namely, anti-symmetric NH_2 stretching -$\nu_{as}(NH_2)$, symmetric NH_2 stretching -$\nu_s(NH_2)$, NH_2 scissoring -$\delta(NH_2)$, NH_2 rocking -$\rho(NH_2)$, NH_2 wagging -$\omega(NH_2)$ and NH_2 torsion-$\tau(NH_2)$ corresponding to the frequencies 3415(ν_2), 3349(ν_3), 1588(ν_{13}), 1108(ν_{31}), 868(ν_{39}) and 290(ν_{60}) cm^{-1} respectively. The modes $\nu_{as}(NH_2)$, $\nu_s(NH_2)$, $\delta(NH_2)$, and $\tau(NH_2)$ were assigned at 3447, 3370, 1605 and 290 cm^{-1} by Govindarasu et al. [31] for the isolated L-PHAL molecule. The anti-symmetric NH_2 stretching -$\nu_{as}(NH_2)$, NH_2 scissoring -$\delta(NH_2)$ are pure and highly localized modes; the symmetric NH_2 stretching-$\nu_s(NH_2)$ is slightly coupled with the $\nu(O_{21}\text{-}H_{22})$ mode in isolated state, the NH_2 torsion-$\tau(NH_2)$ is slightly coupled with the $\tau(C_{19}\text{-}O_{21})$ and $\beta(C_4\text{-}C_{11})$, NH_2 rocking -$\rho(NH_2)$ is slightly coupled with

ω(COOH) and Φ_1(R) while NH_2 wagging -$\omega(NH_2)$ is coupled with $\beta(C_{12}\text{-}C_{19})$.

For the zwitterionic L-TYR molecule the nine modes of vibration due to the NH_3 group as seen from the Gauss View software are: an anti-symmetric NH_2 stretching -$\nu_{as}(NH_2)$, a symmetric NH_2 stretching -$\nu_s(NH_2)$, an NH stretching -ν(NH), two anti-symmetric NH_3 deformations $-\delta_{as}(NH_3)$, the symmetric NH_3 deformation $-\delta_s(NH_3)$, the planar NH_3 rocking $-\rho_2(NH_3)$, the perpendicular NH_3 rocking $-\rho_1(NH_3)$ and the NH_3 torsion-$\tau(NH_2)$ which correspond to the calculated frequencies 3367(ν_2), 3300(ν_3), 2911(ν_9), 1594(ν_{12}), 1549(ν_{16}), 1359(ν_{20}), 1062(ν_{33}), 1035(ν_{34}) and 250(ν_{60}) cm^{-1} respectively. These modes had been assigned at 3295, 3228, 2918, 1623, 1561, 1387, 1105, 1070 and 329 cm^{-1} by Layton et. al. [30] in zwitterionic L-TRYP; at 3204, 3096, 3204, 1459, 1456, 1491, 1104, 1101 and 206 cm^{-1} by Contreras et al. [6] in zwitterionic L-TYR and also at 3366, 3301, 2949, 1585, 1551, 1358, 1030, 900 and 254 cm^{-1} by Dixit et al. [31] in zwitterionic L-PHAL respectively. The anti-symmetric NH_2 stretching -$\nu_{as}(NH_2)$, symmetric NH_2 stretching -$\nu_s(NH_2)$, NH stretching -ν(NH), NH_2 scissoring -$\delta(NH_2)$ are pure and highly localized modes. The NH_3 torsion-$\tau(NH_3)$ is slightly coupled with the $\tau(C_{19}\text{-}O_{21})$ and $\beta(C_4\text{-}C_{11})$.

CH_2 group modes

The six modes of vibrations due to the CH_2 group are assigned at the frequencies 2951(ν_9), 2906(ν_{10}), 1422(ν_{17}), 1234(ν_{24}), 1230(ν_{25}) and 958(ν_{35}) cm^{-1} respectively in the isolated molecule while they have been assigned at the frequencies 2954(ν_{10}), 2910(ν_{11}), 1419(ν_{18}), 1272(ν_{25}), 1181(ν_{28}) and 923(ν_{39}) cm^{-1} respectively in the zwitterionic form. These modes were assigned at the frequencies 2989, 2927, 1436, 1337, 1369 and 906 cm^{-1} by Layton et al. [30] in zwitterionic L-TRYP; at 2856, 2793, 1400, 1590, 1256 and 795 cm^{-1} by Contreras et al. [6] in zwitterionic L-TYR and at 2957, 2911, 1420, 1332, 1086 and 828 cm^{-1} by Dixit et al. [31] in zwitterionic L-PHAL respectively. The $\nu_{as}(CH_2)$, $\nu_s(CH_2)$ and $\delta(CH_2)$ are pure and highly localized modes while $\nu_s(CH_2)$ in isolated molecule is coupled with $\nu(C_{12}\text{-}H_{15})$ and the other modes are strongly coupled with various modes.

HOMO–LUMO energy gap

The HOMO and LUMO are the principal orbitals which are essential in predicting the chemical stability of a molecule [32,36]. The kinetic stability of the molecules is generally expressed in terms of the forbidden energy gap E_g [33,34]. The energy gap of the HOMO and LUMO is a measure of the reactivity of the molecule. The smaller the energy gap more easily it can be excited and vice versa. The smaller HOMO-LUMO energy gap stimulates the eventual ICT interaction taking place within the molecule, which is responsible for the bioactivity of the molecule. The larger value of the energy gap is responsible for the higher kinetic stability and lower chemical reactivity because it would be energetically more difficult to add the electrons to the LUMO and to remove the electrons from the HOMO [35,36]. The schematic diagram of the atomic orbital compositions of the frontier MOs have been shown for isolated and also for the zwitterionic L-TYR molecule in Figure 6. The green and red coloured solid regions in the Figure 6 exhibit the MOs with the completely opposite phases. The present calculations predict the energy gap (E_g), i.e. the transition energy from HOMO to LUMO of the isolated and zwitterionic L-TYR molecule to be 5.60 eV and 4.567 eV.

The Molecule is found to possess a dipole moment 6.11 Debye for isolated state and 12.99 Debye for zwitterionic form, the experimental value of μ=13.95D [6] is in agreement with that of lowest energy conformer of zwitterionic form. The electric polarizability components α_{xx}, α_{xy}, α_{yy}, α_{xz}, α_{yz} and α_{zz} for isolated molecule and zwitterion have been computed as 166.23, -4.68, 120.61, 8.44, 7.08 and 88.00 $Bohr^3$ and 211.73, 5.52, 167.90, -15.54, 12.56 and 124.61 $Bohr^3$, respectively resulting in the net isotropic polarizability 124.94 $Bohr^3$ and 168.08 $Bohr^3$. It is noticeable that both the essential parameters electric dipole moment and electric polarizability significantly higher in the zwitterionic form.

Molecular electrostatic potentials

The molecular electrostatic potentials (MEP) are the essential tools to analyse the inter-molecular association and also the molecular properties of small molecules, actions of the molecules of the drugs and their analogues, the biological functioning of the haemoglobin and enzyme catalysis [35-39]. These are widely utilized as the reactivity map displaying the most probable regions for the electrophilic attack of the point-like charged reagents on the organic molecules [40]. The values and the spatial distribution of the MEPs are generally responsible for the chemical nature of an agent in the chemical reaction. They strongly affect the binding of the substrate to its active site. These potentials would be typically visualized through mapping its values onto the molecular ED. The different values of the MEPs at the surface are represented by different colours; the red colour represents region of the most negative electrostatic potential, the blue colour represents region of the most positive electrostatic potential and the green represents region of zero potential. Potentials occur in the order (MEP)red < (MEP)orange < (MEP)yellow < (MEP)green < (MEP)blue. While the negative electrostatic potential is corresponding to the proton attraction by the concentrated ED in the molecule (and is coloured in shades of red), the positive electrostatic potential is corresponding to the proton repulsion by atomic nuclei in regions where a low ED exists and therefore, the nuclear charge is incompletely shielded (and is coloured in shades of blue). The total density plots and corresponding arrays as well as the MEPs mappings and corresponding arrays for both the considered forms of the L-TYR molecule have been shown in Figure 7. These figures provide a visual demonstration of the chemically active sites and the comparative reactivity of atoms in the molecule. A close investigation of these mappings and arrays predicted that in isolated form of L-TYR the regions nearby each of the functional group, namely, NH_2, COOH and OH groups, provide an active site for neucleo-philic attack, while in zwitterion CO_2 group provide a vast region and OH group provide one site for neucleo-philic attack but no active region has been provided by the NH_3 group.

Analysis on natural orbital bonding

In order to evaluate the electron density distribution amongst the atoms and bonds at the various sites, natural (localized) orbitals are used in computational chemistry. In the localized 1-centre and 2-centre regions of the molecule these generally represent the "maximum occupancy character". The NBOs include the highest possible percentage of the ED, which is ideally close to 2.000, providing the most accurate possible "natural Lewis structure" of the Schrodinger wave function ψ. The high percentage of the ED, often found to be >99% for the common organic molecules, corresponds to an accurate natural Lewis structure.

NBO Interactions: Second order perturbation theory : The natural bond orbitals (NBO) investigation is essential to explain the second-order interactions between the occupied NBOs of one subsystem and unoccupied NBOs of another subsystem, which would be a measure of the intermolecular delocalization or hyper conjugation

[41-46]. The delocalization interaction strengths, E(2), estimated by the second order perturbation theory [31] is given by ,

$$E(2) = \Delta E_{ij} = q_i \frac{F_{ij}^2}{\hat{a}_j - \hat{a}_i}$$

where q_i, E_i, E_j and F_{ij} are donor occupancy, diagonal elements and off diagonal NBO Fock matrix elements.

The interaction energy values between the occupied (donors) i and unoccupied (acceptors) j NBOs, calculated using the second order perturbation theory have been collected in Table 7, Table 8 and Table 9 for isolated and zwitterionic LTYR molecule. The larger value of the interaction energy of the NBOs E(2) signifies more intense interaction between donors and acceptors, i.e. higher the electrons donating tendency from donor to acceptor NBOs. The energy values involved in the hyperconjucative interactions between the carbon atoms in the phenyl ring $\pi (C_1 - C_2)$ $\pi^* (C_3 - C_4)$ and $\pi^* (C_5 - C_6)$, and $\pi (C_3 - C_4) \rightarrow \pi^* (C_1 - C_2)$ and $\pi^* (C_5 - C_6)$, $\pi (C_5 - C_6) \rightarrow \pi^* (C_1 - C_2)$ and $\pi^* (C_3 - C_4)$ are 21.63 and 16.56, 17.85 and 20.93, 22.07 and 18.33 kcal /mole respectively (Table-7) for isolated system while in the zwitterionic state the hyperconjucative binding energy values for the phenyl ring C atoms $\pi (C_2 - C_3)$LP*(1)C_1 and LP(1)C_4, $\pi^*(C_5\text{-}C_6)$ LP*(1)C_1 and LP(1)C_4 have been computed 53.69, 41.08, 54.09 and 44.40 kcal/mole respectively (Table-8). The hyper conjugative interaction and the E_D transfer from the lone pair of the N_{16} atom to the O_{21}-H_{22} orbital in the O_{21}-H_{22}----N_{16} system is found to be present with the energy 10.34 kcal /mole in the isolated molecule while the interaction and ED transfer from the lone pair of the O_{21} atom to N_{16}-H_{24} orbital in the N_{16}-H_{24}.....O_{21} system appears to be present with the interaction energy 14.22 kcal /mole in zwitterion. Obviously, stronger intramolecular H bonding exists in the zwitterionic system than isolated system. The intramolecular hydrogen bonding would be possible by the orbital overlapping between LP (1) N_{16} and π^* (O_{22}-H_{22}) in isolated system and similarly for zwitterion it would be due to orbital overlapping between LP(2)O_{21} and σ^* (N_{16}-H_{24}), which may cause intramolecular charge transfer (ICT) giving rise to the stabilization of the hydrogen bonded system [47]. Of course, the hydrogen bonding interaction leads to increase in the electron density (E_D) of O_{21}-H_{22} as well as N_{16}-H_{24} non-Lewis orbital in the two species of L-TYR. Clearly, the energy values involved in the hyper conjugative interaction LP (1) $N_{16} \rightarrow \pi^* (O_{21} - H_{22})$ and LP (2) $O_{21} \rightarrow \sigma^*(N_{16}\text{-}H_{24})$ are 10.34 and 14.22 kcal / mole. The other strong electron lone pair interactions are LP (1) $O_{20} \rightarrow$ RY* (1) C_{19}, LP (2) $O_{20} \rightarrow \sigma^* (C_{12} - C_{19})$, LP (2) $O_{20} \rightarrow \sigma^* (C_{19} - O_{21})$ and LP (2) $O_{21} \rightarrow \pi^* (C_{19} - O_{20})$ resulting in the stabilization energy of about 17.90, 19.05, 31.61 and 48.56 kcal/ mole in the isolated system while in zwitterion LP(1) $C_4 \rightarrow \pi^* (C_2 - C_3)$ and $\pi^* (C_5 - C_6)$, LP(2) $O_{20} \rightarrow \sigma^*(C_{12}\text{-}C_{19})$ and $\sigma^*(C_{19}\text{-}O_{21})$, LP(2) $O_{21} \rightarrow \sigma^*(C_{12}\text{-}C_{19})$ and $\sigma^*(C_{19}\text{-}O_{20})$, LP(3) $O_{21} \rightarrow \pi^*(C_{19}\text{-}O_{20})$ and LP(2) $O_{22} \rightarrow$ LP*(1)C_1 possess stabilization energies 77.03, 75.71, 20.63, 20.31, 16.37, 17.87, 95.87 and 49.41 kcal/mole. It is interesting to note that in the present isolated molecular system, the non Lewis donor to non Lewis acceptor interactions $\pi^*(C_1\text{-}C_2) \rightarrow \pi^*(C_3\text{-}C_4)$ and $\pi^*(C_5\text{-}C_6)$ exist with the higher interaction energies about 266.58 and 289.41respectively. Clearly, $\pi^*(C_1\text{-}C_2)$ a non Lewis NBO conjugated with the $\pi^*(C_5\text{-}C_6)$ resulting to the highest stabilization of 289.41 kcal/mole.

Conclusions

The optimised structures of the most stable conformers of the L-TYR molecule in two different phases have been investigated. These are found to have C_1 symmetry. The r(N_{16}-H_{24}) bond length have been found exceptionally larger and the bond angle $\alpha(N_{16}\text{-}C_{12}\text{-}C_{19})$ much shorter than the observed values in the zwitterion indicating the presence of intramolecular interaction. The natural, APT and Mulliken partial atomic charges at different sites of the lowest energy conformers in both the phases have been discussed. The C atom belonging to the COOH/ CO_2 group possesses the largest magnitude of the APT atomic charge (1.156077e/ 1.677125e) due to presence of the O_{20} atom. The H atoms of the CH_2 group have the smallest magnitude (0.001787e/ 0.000283e) for isolated and zwitterionic phases. The atoms C_4 and C_2 attain the highest and lowest values of the Mulliken atomic charges. The IR and Raman vibrational frequencies and the corresponding intensities of the most stable conformers of both the species have been computed using the DFT-B3LYP/ 6-311++G** method. The computed vibrational fundamentals have been found to be in agreement with the experimentally observed frequencies. The values of the observed and the scaled wave numbers are close to each other. The presence of the IR band at 2075 cm^{-1} is an indicative of the presence of the molecule in the zwitterionic form. The intramolecular H bonding O_{21}-H_{22}----N_{16} in isolated form and N_{16}-H_{24}.....O_{21} in zwitterion have been confirmed by the geometrical, vibrational and NBO analysis. The overlapping between the NBOs LP (1) N_{16} and π^* (O_{21}-H_{22}) in the isolated form and between the NBOs LP (2) O_{21} and σ^* (N_{16}-H_{24}) in the zwitterionic form causes the intramolecular charge transfer (ICT) and also the stabilization of the H bonded system. The HOMO – LUMO energies reveal the ICT interaction between the donor and acceptor NBOs groups. The MEPs plots predict that in the isolated form of L-TYR the regions nearby each functional group NH_2/COOH /OH provide an active site for neucleo-philic attack, while in zwitterion CO_2 group provide a vast region and OH group provide a site for neucleo-philic attack but no active region has been found in the neighbourhood of the NH_3 group. The molecule is found to possess a permanent dipole moment and isotropic polarizability having the values 6.1104 Debye and 124.94 $Bohr^3$ respectively in the isolated state but 12.99 Debye and 168.08 $Bohr^3$ respectively in the zwitterionic form. The material of the molecule is also found to be diamagnetic.

References

1. Bhowon MG, Jhaumeer-Laulloo S, Wah HLK, Ramasami P (2012) Chemistry for Sustainable Development, Springer Dordrecht Heidelberg, London, New York, pp: 81-102.
2. Skerget M, Kotnik P, Hadolin M, Hras AR, Simonic M, et al. (2005) Phenols, proanthocyanidins, ?avones and ?avonols in some plant materials and their antioxidant activities. Food Chem 89: 191-198.
3. Gulcin I (2007) Comparison of in vitro antioxidant and antiradical activities of L-tyrosine and L-Dopa. Amino Acids 32: 431-438.
4. Kecel S, Ozel A E, Akyuz S, Celik S, Agaeva G (2011) Conformational analysis and vibrational spectroscopic investigation of L-proline–tyrosine (L-Pro–Tyr) dipeptide. J Mol Str 993: 349-356.
5. Ramaekers R, Pajak J, Rospenk M, Maes G (2005) Matrix-isolation FT-IR spectroscopic study and theoretical DFT(B3LYP)/6-31++G** calculations of the vibrational and conformational properties of tyrosine. Spectrochim Acta A Mol Biomol Spectrosc 61: 1347-1356.
6. Contreras CD, Ledesma AE, Lanus HE, Zinczuk J, Brandan SA (2011) Hydration of l-tyrosine in aqueous medium. An experimental and theoretical study by mixed quantum mechanical/molecular mechanics methods. Vibrational Spectroscopy 57: 108-115.
7. Gelenberg AJ, Gibson CJ, Wojcik JD (1982) Neurotransmitter precursors for the treatment of depression. Psychopharmacol Bull 18: 7-18.
8. Meyer JS, Welch KM, Deshmukh VD, Perez FI, Jacob RH, et al. (1977) Neurotransmitter precursor amino acids in the treatment of multi-infarct dementia and Alzheimer's disease. J Am Geriatr Soc 25: 289-298.
9. Deijen JB, Wientjes CJ, Vullinghs HF, Cloin PA, Langefeld JJ (1999) Tyrosine improves cognitive performance and reduces blood pressure in cadets after one week of a combat training course. Brain Res Bull 48: 203-209.

10. Mongan J, Case DA, McCammon JA (2004) Constant pH molecular dynamics in generalized Born implicit solvent. J Comput Chem 25: 2038-2048.

11. Fang L, Zhang H, Cui W, Ji M (2008) Studies of the mechanism of selectivity of protein tyrosine phosphatase 1B (PTP1B) bidentate inhibitors using molecular dynamics simulations and free energy calculations. J Chem Inf Model 48: 2030-2041.

12. Hu X, Stebbins CE (2006) Dynamics of the WPD loop of the Yersinia protein tyrosine phosphatase. Biophys J 91: 948-956.

13. Mostad A, Nissen HM (1971) The structure of l-tyrosine. Tetrahedron Lett 12: 2131-2132.

14. Frey MN, Koetzle TF, Lehmann MS, Hamilton WC (1973) Precision neutron diffraction determination of protein and nucleic acid components. I. The crystal and molecular structure of the amino acid L-alanine. J Am Chem Soc 58: 2657-2660.

15. Goodwill KE, Sabatier C, Marks C, Raag R, Fitzpatrick-Raymond PF, et al. (1997) Crystal structure of tyrosine hydroxylase at 2.3 Å and its implications for inherited neurodegenerative diseases. Nat Struct Biol 4: 578-585.

16. Antson AA, Demidkina TV, Gollnick P, Dauter Z, von Tersch RL, et al. (1993) Three-dimensional structure of tyrosine phenol-lyase. Biochemistry 32: 4195-4206.

17. Yang J, Liu L, He D, Song X, Liang X, et al. (2003) Crystal structure of human protein-tyrosine phosphatase SHP-1. J Biol Chem 278: 6516-6520.

18. Mohammadi M, Froum S, Hamby JM, Schroeder MC, Panek RL, et al. (1998) Crystal structure of an angiogenesis inhibitor bound to the FGF receptor tyrosine kinase domain. EMBO J 17: 5896-5904.

19. Suga T, Inubushi C, Okabe N (1998) O-Phospho-L-tyrosine. Acta Crystallogr C 54: 83-85.

20. Broermann A, Steinhoff HJ, Schlücker S (2014) Towards label-free and site-specific probing of the local pH in proteins: pH-dependent deep UV Raman spectra of histidine and tyrosine. J Mol Str 1073: 77-81.

21. Wojciechowska A, Kochel A, Komorowska M (2011) Synthesis, crystal structure and spectroscopy studies of a novel five-coordinated Zn(II) ion complex with L-tyrosine and imidazole. Polyhedron 30: 2361-2367.

22. Fischer WB, Eysel HH (1997) Raman and FTIR spectroscopic study on water structural changes in aqueous solutions of amino acids and related compounds. J Mol Str 415: 249-257.

23. Grace LI, Cohen R, Dunn TM, Lubman DM, de Vries MS (2002) The R2PI Spectroscopy of Tyrosine: A Vibronic Analysis. Journal of Molecular Spectroscopy 215: 204-219.

24. Ojha AK (2007) pH dependent SERS and solvation studies of tyrosine adsorbed on silver colloidal nano particles combined with DFT calculations. Chemical Physics 340: 69-78.

25. Dixit V, Yadav RA (2015) Experimental IR and Raman Spectroscopy and DFT Methods Based Material Characterization and Data Analysis of 2- Nitrophenol. Biochem Pharmacol (Los Angel) 4: 183.

26. Frisch MJ, Trucks GW, Schlegel HB, Scuseria GE, Robb MA, et al. (2010) Gaussian 09, Revision C.01, Gaussian, Inc., allingford, CT.

27. Dixit V, Yadav RA (2015) DFT-B3LYP computations of electro and thermo molecular characteristics and mode of action of fungicides (chlorophenols). Int J Pharm 491: 277-284.

28. Dixit V, Yadav RA (2015) Structural and vibrational studies of some pesticides: 2-chlorophenol,2,4,6-trichlorophenol and pentachlorophenol. Asian Journal of Physics 24.

29. Martin JML, Van Alsenoy C (1995) GAR2PED, A Program to Obtain a Potential Energy Distribution from a Gaussian Archive Record, University of Antwerp, Belgium.

30. Rauhut G, Pulay P (1995) Transferable Scaling Factors for Density Functional Derived Vibrational Force Fields. J Phys Chem 99: 3093-3100.

31. Govindarasu K, Kavitha E (2014) Molecular structure, vibrational spectra, NBO, UV and firrst order hyperpolarizability, analysis of 4-Chloro-DL-phenylalanine by density functional theory. Spectrochimica Acta Part A 133: 799-810.

32. Dewar MJS (1969) The Molecular Orbital Theory of Organic Chemistry. McGraw-Hill and Inc.

33. Charles Alfred Coulson, McWeeny R (1979) Coulson's Valence. Oxford University Press.

34. Ferreira MMC, Suto E (1992) Atomic polar tensor transferability and atomic charges in the fluoromethane series. J Phys Chem 96: 8844-8849.

35. Leyton P, Brunet J, Silva V, Paipa C, Castillo MV, et al. (2012) An experimental and theoretical study of L-Tryptophan in an aqueous solution, combining two-layered ONIOM and SCRF calculations. Spectrochim Acta A Mol Biomol Spectrosc 88: 162-170.

36. Dixit V, Yadav RA, Yogesh M, Santhosh C (2015) Experimental IR and Raman and DFT methods based spectroscopic and electronic chracterization of L-phenylalanine in isolated and zwitterionic forms. Vib Spectrosc.

37. Gunasekaran S, Balaji RA, Kumaresan S, Anand G, Srinivasan S (2008) Experimental and theoretical investigations of spectroscopic properties of N-acetyl-5-methoxytryptamine. Can J Anal Sci Spectrosc 53: 149-160.

38. Foresman JB, Frisch AE (1996) Exploring Chemistry with Electronic Structure Methods (2nd edn) Gaussian, Pittsburgh, PA.

39. Lewars E (2003) Computational Chemistry—Introduction to the Theory and Applications of Molecular and Quantum Mechanics, Kluwer Academic Publishers, Norwell, MA.

40. Manolopoulos DE, May JC, Down SE (1991) Theoretical studies of the fullerenes: C34 to C70. Chem Phys Lett 181: 105-111.

41. Politzer P, Truhlar D (1981) Chemical Application of Atomic and Molecular Electrostatic Potentials, Plenum, New York pp: 257-294.

42. Moro S, Bacilieri M, Ferrari C, Spalluto G (2005) Autocorrelation of molecular electrostatic potential surface properties combined with partial least squares analysis as alternative attractive tool to generate ligand-based 3D-QSARs. Curr Drug Discovery Technol 2: 13-21.

43. Murray JS, Sen K (1996) Molecular Electrostatic Potentials: Concepts and Applications, Elsevier, Amsterdam.

44. Weiner PK, Langridge R, Blaney JM, Schaefer R, Kollman PA (1982) Electrostatic potential molecular surfaces. Proc Natl Acad Sci U S A 79: 3754-3758.

45. Politzer P, Truhlar DG (1981) Chemical Application of Atomic and Molecular Electrostatic Potentials, Plenum, New York.

46. James C, Amalraj A, Reghunathan R, Joe IH, Jayakumar VS (2006) Structural conformation and vibrational spectroscopic studies of 2,6-bis(p-N,N-dimethyl benzylidene) cyclohexanone using density functional theory. J Raman Spectrosc 37: 1381-1392.

47. Liu JN, Chen ZR, Yuan SF (2005) Study on the prediction of visible absorption maxima of azobenzene compounds. J Zhejiang Univ Sci B 6: 584-589.